NAT'L INST. OF STAND & TECH R.I.C.
A11105 043095
NIST
PUBLICATIONS

NISTIR 5880

Mathematical Analysis of Practices to Control Moisture in the Roof Cavities of Manufactured Houses

D. M. Burch
Building and Fire Research Laboratory
Gaithersburg, Maryland 20899-0001

G. A. Tsongas
Mechanical Engineering Department
Portland State University
Portland, Oregon 97207

G. N. Walton
Building and Fire Research Laboratory
Gaithersburg, Maryland 20899-0001

United States Department of Commerce
Technology Administration
l Institute of Standards and Technology

QC
100
.U56
NO.5880
1996

NISTIR 5880

Mathematical Analysis of Practices to Control Moisture in the Roof Cavities of Manufactured Houses

D. M. Burch, G.A. Tsongas, and G.N. Walton

September 1996
Building and Fire Research Laboratory
National Institute of Standards and Technology
Gaithersburg, Maryland 20899

U.S. Department of Commerce
Michael Kantor, *Secretary*
Technology Administration
Mary L. Good, *Under Secretary for Technology*
National Institute of Standards and Technology
Arati Prabhakar, *Director*

Prepared for:
U.S. Department of Housing And Urban Development
Washington, D.C. 20410

TABLE OF CONTENTS

LIST OF TABLES

LIST OF FIGURES

ABSTRACT

A mathematical model is presented that predicts moisture and heat transfer in ventilated cavities such as attics, roof cavities, and cathedral ceilings. The model performs a transient moisture and heat balance as a function of time of year and includes the storage of moisture and heat at the construction layers. The model includes both molecular diffusion and capillary transfer within the materials. Radiation exchange among the ventilated cavity surfaces is predicted using a mean-radiant-temperature-network model. Latent heat (i.e., the effect of water evaporating from one place and condensing at another place) is distributed within the materials. Airflow from the house into the ventilated cavity is predicted using a stack effect model with aggregated effective leakage areas. Air exchange between the ventilated cavity and outdoor environment is predicted by a semi-empirical model. The relative humidity in the house is permitted to vary during the winter and is calculated from a moisture balance of the whole building.

This mathematical model was used to simulate the performance of a double-wide manufactured house constructed in compliance with the latest HUD Standards. An interior vapor retarder was installed in the ceiling construction and ventilation openings were installed in the roof cavity consistent with the 1/300 rule given in the HUD Standards. The effect of passive and mechanical ventilation, as well as a wide range of other factors on the roof sheathing moisture content was investigated as a function of time. The weekly average moisture content of the lower surface of the plywood sheathing was analyzed in several cold climates, while the relative humidity at the lower surface of the ceiling insulation was analyzed in a hot and humid climate.

The analysis revealed the following: 1) airflow from the house into the roof cavity, as opposed to water-vapor diffusion, was the dominant moisture transport mechanism into the roof cavity; 2) high roof sheathing moisture content occurred in houses having high indoor relative humidity (i.e., high moisture production rate, or tight construction, or both); 3) passive roof cavity vents consistent with the 1/300 rule were found to maintain the roof sheathing moisture content in non-humidified houses below fiber saturation during the winter; 4) the mechanical roof cavity ventilation rate specified in the HUD Standards for removing moisture during the winter was found to be too small and thus needs to be revised; 5) the presence of a ceiling vapor retarder was found to provide very small reductions in roof sheathing moisture content; 6) when an interior vapor retarder was installed in the ceiling construction of an air-conditioned house exposed to a hot and humid climate, the relative humidity at its upper surface rose above 80%, thereby providing a conducive environment for mold and mildew growth; and 7) the use of ceiling vents to provide additional whole house ventilation in cold climates substantially increased the roof sheathing moisture content of a house with an unventilated attic. Recommendations for further study are presented.

KEYWORDS

Airflow, Attic Ventilation, Attics, Building Technology, Ceiling Vents, Guidelines and Practices, HUD Standards, Manufactured Housing, Mathematical Analysis, Moisture, Moisture Analysis, Moisture Control, Moisture Modeling, Roof Cavities and Roof Ventilation.

INTRODUCTION

During the winter, moisture released by occupant activities causes the absolute humidity (or water vapor pressure) inside a manufactured house to be higher than that of the outdoor air. This vapor pressure potential causes water vapor to diffuse through the ceiling construction into the roof cavity. In addition, a buoyant force (i.e., the stack effect) causes airflow from the house into the roof cavity[1] through cracks and penetrations (e.g., ceiling light fixtures, plumbing and HVAC penetrations, and cracks above interior partition walls). A portion of this moisture is removed by attic ventilation. The remainder becomes absorbed or condenses onto the cold interior surfaces of the roof cavity (most important of which is the plywood roof sheathing).

It is possible for the moisture content of the roof sheathing to rise above fiber saturation (e.g., 28% moisture content for plywood). Above fiber saturation, wood decay can occur. However, the wood must be warm {above 10 °C (50 °F) and optimally between 24 °C (75 °F) and 32 °C (90 °F)} (Sherwood 1994). Concerns regarding the possibility of decay tend to be worse in manufactured houses because they tend to have higher indoor relative humidity compared to site-built houses. This is because they are tighter (Hadley and Bailey 1990) and have smaller interior volumes than site-built houses.

In an effort to prevent roof cavity moisture problems, the Department of Housing and Urban Development (HUD) issued rules in their Manufactured Home Construction and Safety Standards (U.S. Department of Housing and Urban Development 1994). Henceforth in this report, these standards will be referred to as the HUD Standards. The rules require manufactured houses to have an interior ceiling vapor retarder, except for houses constructed in the southeastern part of the United States where a ceiling vapor retarder is optional. In addition, houses constructed with moisture absorbing roof sheathing are required to be provided with either a passive or mechanical attic ventilation for removing moisture from their roof cavities. Passive attic ventilation systems shall have a net free ventilation opening of 1/300 of the attic floor area. Mechanical attic ventilation systems shall provide a minimum air change rate of 0.00010 m^3/s per m^2 (0.02 ft^3/min per ft^2) of attic floor area. Single-wide houses constructed with metal roofs are not required to have attic ventilation.

Providing an interior vapor retarder in the ceiling construction and ventilating the roof cavity may be counter-productive and actually cause a summer moisture problem in manufactured houses located in hot and humid climates. This is because the attic ventilation airflow transports a large amount of moisture into the roof cavity from the outdoors. This moisture subsequently diffuses downward through the insulation to the upper surface of the vapor retarder which may be cooled by the indoor air conditioning equipment below the dew point temperature of the roof cavity air. In this situation, condensation occurs and the relative humidity at the upper surface of the vapor retarder approaches a saturated state, thereby providing a conducive environment for mold and mildew

---

[1] In this report, the attic of a manufactured house is referred to as a "roof cavity" in order to emphasize that it generally has a smaller volume with less ventilation clearance than a site-built house.

growth. A monthly mean surface relative humidity greater than 80% is conducive to mold and mildew growth (International Energy Agency 1990). Once mold and mildew exists, fungal spores may enter the living space and cause indoor air quality and health-related problems (Olson, J., Schooler, S., and Mansfield, M. 1993).

A transient heat and moisture transfer model (Burch and Thomas 1991), developed at the National Institute of Standards and Technology (NIST) and called MOIST, was recently used to analyze the effectiveness of various moisture control practices for the roof cavities of manufactured housing. In that previous study (Burch 1995), it was found that a combination of passive measures consisting of a ceiling vapor retarder, sealing air leakage sites in the ceiling construction, and providing attic ventilation openings maintained the moisture content of the roof sheathing well below fiber saturation. However, the version (2.1) of the MOIST model used in that study had several important limitations that likely influenced the results. First, the indoor relative humidity in the house below had to be held constant during the simulation. In actual houses, the indoor relative humidity varies considerably throughout the year and that can influence moisture content results substantially (Tsongas, Burch, Roos, and Cunningham 1995). Second, the stack effect airflow from the house into the roof cavity was treated as constant. In practice, this airflow will tend to vary with the time of year. And third, the attic ventilation rate was taken to be constant during the simulation. In practice, the attic ventilation rate varies as a function of the outdoor wind speed.

Because of the above limitations, it was decided to modify the model to remove the limitations. In the present study, a more comprehensive model is presented that allows analysis without the above limitations. The model is used to simulate the performance of a current practice double-wide manufactured house. Various factors that affect the moisture content of the roof sheathing are analyzed. The effectiveness of the current moisture control practices specified within the HUD Standards are investigated in several cold climates and a hot and humid climate.

THEORY

Assumptions

Some of the more important assumptions of the new roof cavity moisture and heat transfer model are given below:

- Moisture and heat transfer are one-dimensional;
- Air within the ventilated cavity is well mixed; and
- The wetting of exterior surfaces by rain is neglected, and the insulating effect and change in roof absorptance from a snow load are neglected.

Other assumptions are discussed in the model presentation below.

Basic Transport Equations

The basic transport equations are taken from Pedersen (1990) and are briefly presented below. Within each material of the construction, the moisture distribution is governed by the following conservation of mass equation:

$$\frac{\partial}{\partial y}(\mu\frac{\partial p_v}{\partial y}) - \frac{\partial}{\partial y}(K\frac{\partial p_l}{\partial y}) = \rho_d\frac{\partial \gamma}{\partial t} \quad (1)$$

Symbols are defined in the Nomenclature at the end of the report. The first term on the left side of Equation 1 represents water-vapor diffusion, whereas the second term represents capillary transfer. The right side of Equation 1 represents moisture storage within the material. The minus sign accounts for the fact that liquid flows in a porous material in the same direction as the gradient in capillary pressure. The sorption isotherm (i.e., the relationship between equilibrium moisture content and moisture content) and the capillary pressure curve (i.e., the relationship between capillary pressure and moisture content) were used as constitutive relations in solving Equation 1.

The temperature distribution is calculated from the following conservation of energy equation:

$$\frac{\partial}{\partial y}(k\frac{\partial T}{\partial y}) + h_{lv}\frac{\partial}{\partial y}(\mu\frac{\partial p_v}{\partial y}) = \rho_d c\frac{\partial T}{\partial t} \quad (2)$$

The first term on the left side of Equation 2 represents conduction, whereas the second term is the latent heat transfer derived from any phase change associated with the movement of moisture. The right side of Equation 2 represents the storage of heat within a material.

In Equation 1, the water vapor permeability (μ) and the hydraulic conductivity (K) are strong functions of moisture content. In Equation 2, the thermal conductivity (k) is also a function of moisture content, but for the present analysis it is assumed to be constant.

Ventilated Cavity Moisture and Heat Balance

Applying the principle of conservation of mass to a ventilated cavity, the sum of the evaporation rate from the ventilated cavity surfaces plus the rate of moisture transfer by airflow from the house into the cavity is equal to the rate of moisture removed by outdoor ventilation, or:

$$\sum_{n=1}^{N} A_n m_n (p_{v,n} - p_{v,c}) + \rho_a \dot{V}_{h\to c}(\omega_i - \omega_c) = \rho_a \dot{V}_c(\omega_c - \omega_o) \quad (3)$$

In a similar fashion, the principal of conservation of energy may be applied to the cavity air volume.

The net rate of convective heat transfer from the cavity surfaces plus the rate of energy transfer by airflow from the house into the cavity is equal to the rate of energy removed by outdoor ventilation, or:

$$\sum_{n=1}^{N} A_n h_{c,n}(T_{s,n} - T_c) + \rho_a c \dot{V}_{h\to c}(T_i - T_c) = \rho_a c \dot{V}_c(T_c - T_o) \qquad (4)$$

Radiation exchange among the ventilated cavity surfaces is handled using the mean-radiant-temperature network method described by Carrol (1980).

Airflow from House into Attic

The airflow rate from the house into the roof cavity is predicted using the equation (ASHRAE 1993):

$$\dot{V}_{h\to c} = L_e \sqrt{\frac{(2\Delta p_r)}{\rho_a}} \left(\frac{\Delta p_t}{\Delta p_r}\right)^{0.65} \qquad (5)$$

Airflow passes through the following three leakage areas: the ceiling, the roof, and the house below. The effective leakage area of the series combination of the three areas is given by the relation:

$$L_e = \left[\left(\frac{1}{L_w}\right)^{1/0.65} + \left(\frac{1}{L_c}\right)^{1/0.65} + \left(\frac{1}{L_r}\right)^{1/0.65} \right]^{-0.65} \qquad (6)$$

Here the effective leakage area for each of the house parts has been aggregated at a single location placed at the mid-height level of each part. The total stack-effect pressure head (Δp_t) is equal to the sum of the pressures for the house and the roof cavity, or:

$$\Delta p_t = \rho_a H_h \left(\frac{T_i - T_o}{T_o}\right) + \rho_a H_c \left(\frac{T_c - T_o}{T_o}\right) \qquad (7)$$

The first and second terms are the house and roof cavity stack effect pressures, respectively.

The NIST Contaminant Air Flow Model (Walton 1994) was used to investigate the validity of the assumption of aggregating the wall effective leakage area (ELA) at a single location at the mid-

height level. For the investigation, the stack-effect airflow from the house into the roof cavity was predicted for two cases. In the first case, the wall ELA was equally distributed into eight separate ELA's spaced at equal intervals from the floor to the ceiling. In the second case, the wall ELA was aggregated at a single location at the mid-height level. The two simulations agreed within 9%, thereby supporting the validity of the simplifying assumption.

Roof Cavity Ventilation Rate

The single-zone infiltration model developed by Sherman and Grimsrud (1980) was applied to estimate the air exchange rate between a roof cavity and the outdoor environment, or:

$$\dot{V}_c = L_r \left[C_{\Delta T,c} |T_c - T_o| + C_{v,c} v^2 \right]^{0.5} \quad \textbf{(8)}$$

The coefficients ($C_{\Delta T,c}$ and $C_{v,c}$) were evaluated by fitting the above equation to a set of measured data, as described in a later section.

Indoor Boundary Conditions

At the indoor surface of the construction, the moisture transfer through an air film and paint layer (or wallpaper) is equated to the diffusion transfer into the solid material surface, or:

$$M_{e,i}(p_{v,i} - p_v) = -\mu \frac{\partial p_v}{\partial y} \quad \textbf{(9)}$$

where the quantities are evaluated at the indoor surface. Here, an effective conductance ($M_{e,i}$), defined by:

$$M_{e,i} = \frac{1}{\frac{1}{M_{f,i}} + \frac{1}{M_{p,i}}} \quad \textbf{(10)}$$

has been introduced. The effect of a thin paint layer is taken into account as a surface conductance ($M_{p,i}$) in series with the convective mass transfer coefficient ($M_{f,i}$) associated with the air film.

At the same boundary, the heat transferred through the air film, ignoring the thermal resistance of the paint layer, is equated to the heat conducted into the indoor surface, giving:

$$(h_{r,i} + h_{c,i})(T_i - T) = -k\frac{\partial T}{\partial y} \quad \textbf{(11)}$$

where all quantities are evaluated at the indoor surface.

Outdoor Boundary Conditions

At the outdoor surface of the construction, a set of equations similar to Equations 9 and 10 were applied to compute the moisture transfer. The heat conducted into the outdoor surface and the absorbed solar radiation is set equal to the heat loss to the outdoor air by convection and thermal radiation between the surface and sky, or:

$$-k\frac{\partial T}{\partial y} + \alpha H_{sol} = h_{c,o}(T - T_o) + h_{r,o}(T - T_{sky}) \quad \textbf{(12)}$$

where all quantities are evaluated at the outdoor surface. Here $h_{r,o}$ is the radiative heat transfer coefficient defined by the relation:

$$h_{r,o} = 4E\sigma T_m^3 \quad \textbf{(13)}$$

where E is the emittance factor which includes the surface emissivity and the view factor from the outdoor surface to the sky and T_m is the mean temperature between the surface and the sky. The solar radiation (H_{sol}) incident onto exterior surfaces having arbitrary tilt and orientation was predicted using algorithms given in Duffie and Beckman (1991). The sky temperature was calculated using an equation developed by Bliss (1961).

Indoor Temperature and Humidity Conditions

Space Heating Operation. When the daily average outdoor temperature is less than or equal to the balance point temperature for space heating, the house operates in a space heating mode. The indoor temperature is taken to be equal to the heating set point temperature. The indoor relative humidity is permitted to vary and is calculated from a moisture balance of the whole building.

The rate of moisture production by the occupants is equal to the rate of moisture removed by natural and /or forced ventilation plus the rate of moisture storage at interior surfaces and furnishings, or:

$$\dot{W} = \rho_a \dot{V}_{h,t}(\omega_i - \omega_o) + \kappa A_f(\phi_i - \phi_{i,\tau}) \quad \textbf{(14)}$$

The sorption constant per unit floor area (κ) must be determined from a whole house experiment (see TenWolde 1994). Using the psychrometric relationship between humidity ratio (ω) and relative humidity (ϕ) as a constitutive relation, the above equation may be solved for the indoor relative humidity.

The hygric memory ($\phi_{i,\tau}$) is computed from the relation:

$$\phi_{i,\tau} = \frac{\sum_{n=N-4\tau}^{N-1} Z(n)\phi_i(n)}{\sum_{n=N-4\tau}^{N-1} Z(n)} \qquad \textbf{(15)}$$

The exponential weighting factors Z(n) are defined as:

$$Z(n) = e^{-(N-n)/\tau} \qquad \textbf{(16)}$$

In the hourly calculations, the dew point temperature of the indoor air is compared with the temperature of the inside glass surface to determine if condensation occurs. When condensation occurs, the vapor pressure of the indoor air is taken to be equal to the saturation pressure at the inside glass surface. The indoor relative humidity is calculated from the indoor temperature and vapor pressure using psychrometric relationships.

The natural ventilation rate for the house is predicted by the single-zone Lawrence Berkeley Laboratory (LBL) Infiltration Model developed by Sherman and Grimsrud (1980) and described by ASHRAE (1993) which is given by:

$$\dot{V}_{h,n} = L_h \left[C_{\Delta T,h} |T_i - T_o| + C_{v,h} v^2 \right]^{0.5} \qquad \textbf{(17)}$$

When mechanical ventilation $V_{h,m}$ is present, the total ventilation rate $V_{h,t}$ in Equation (14) is determined by the relation (Palmiter and Bond 1991):

$$\begin{aligned} &\text{If } \dot{V}_{h,m} < 2\dot{V}_{h,n}, \quad \dot{V}_{h,t} = \dot{V}_{h,n} + 0.5\, \dot{V}_{h,m} \\ &\text{If } \dot{V}_{h,m} \geq 2\dot{V}_{h,n}, \quad \dot{V}_{h,t} = \dot{V}_{h,m} \end{aligned} \qquad \textbf{(18)}$$

It should be noted that in Equation 18, $V_{h,m}$ is the actual mechanical ventilation rate produced by the

ventilation equipment installed in the house, as opposed to the rated value. The actual value is typically about half of the rated value (Tsongas 1990).

Space Cooling Operation. When the daily average outdoor temperature is greater than or equal to the balance point temperature for space cooling, the house operates in a space cooling mode. The indoor temperature and relative humidity are maintained at constant specified values.

Floating Operation. When the daily average outdoor temperature is greater than the balance point for space heating and less than the balance point for space cooling, then neither space heating nor space cooling are required, it is assumed that the windows are opened, and the indoor temperature and relative humidity are equal to the outdoor values. When the space cooling equipment is turned off, it was assumed that the occupant will open the windows, and the building again operates in a well ventilated mode.

Solution Procedure

A FORTRAN 77 computer program, called the MOIST Attic Model, was prepared to solve the above system of equations. Finite-difference equations were developed to represent the basic moisture and heat transport equations (Eqs. 1 and 2).

The solution of the complete system of equations proceeded by first solving for the all material temperatures and the cavity air temperature. A flow chart describing the steps of the thermal solution is given in Figure 1. Since the material temperatures and the cavity air temperature are dependent upon one another, it is necessary to iteratively solve at each time step the material temperatures and cavity air temperature until convergence is achieved.

The model next solves for the water vapor pressure distribution within the materials and the cavity water vapor pressure. A flow chart describing the steps of the moisture solution is given in Figure 2. Since the material vapor pressures and the cavity vapor pressure are dependent on one another, it is necessary to iteratively solve at each time step the material vapor pressures and cavity vapor pressure until convergence is attained. The model next solves for the distribution of capillary pressures within the materials. From the predicted gradients in vapor pressure and capillary pressure and the transport coefficients for vapor and liquid flows, a new set of material moisture contents is calculated. The model is now ready to proceed to the next time step.

Before making the final computer runs for the present study, a series of special computer runs were carried out to establish that the finite-difference representation of the transport equations was indeed converging. In a sequence of simulations, the number of the finite-difference nodes in each material was doubled until no further change in the solution occurred.

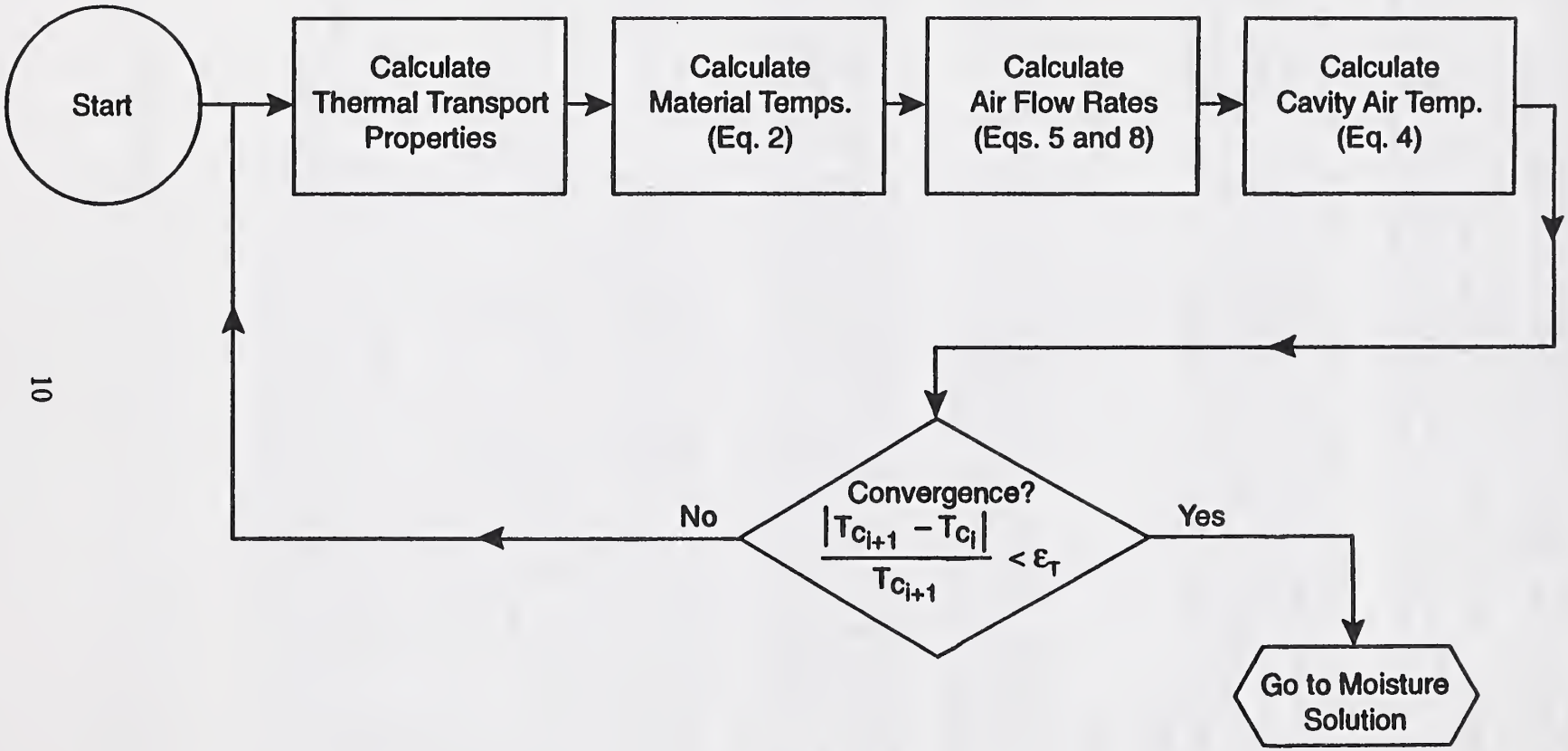

Fig. 1. Flow chart of thermal solution.

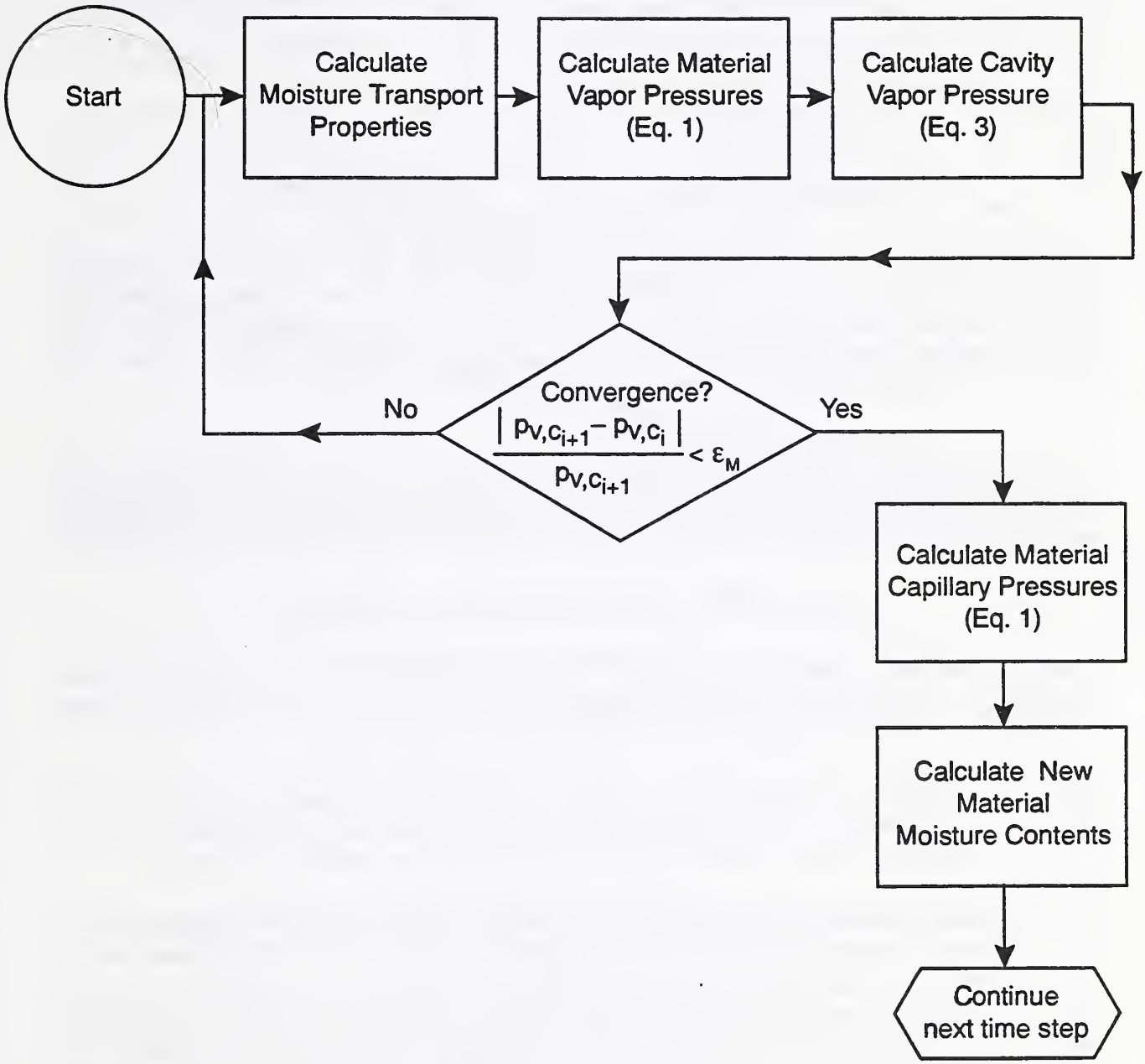

Fig. 2. Flow chart of moisture solution.

The number of finite-difference nodes used in the roof construction, which is the focus of the analysis, is given in Table 1 below.

Table 1. Number of Finite-Difference Nodes in Roof Construction		
Construction Layer	Thickness, mm (in.)	Nodes
Thin Surface Layer, Plywood Roof Sheath.	1.3 (0.050)	2
Remainder Layer, Plywood Roof Sheath.	10.6 (0.419)	5
Building Paper	0.79 (0.031)	2
Asphalt Roof Shingles	6.4 (0.25)	2

Dividing the plywood into two separate layers (i.e., a thin surface layer and a remainder layer) is a trick used to achieve convergence of the mathematical solution with a fewer number of nodes. This also allowed determination of the moisture content of the plywood sheathing adjacent to the cavity. A similar number of nodes were used in the other construction components. The thin surface layer should have the highest moisture content of the sheathing.

In another set of simulations, the convergence criteria for the thermal solution (ϵ_T) and the convergence criteria for the moisture solution (ϵ_M) were decreased until no further change in the solution occurred. A value of 1.0×10^{-4} for ϵ_m and ϵ_T provided convergence of the mathematical solution.

DESCRIPTION OF CURRENT PRACTICE HOUSE

In selecting the construction of the current practice house, the authors contacted manufacturers and other persons knowledgeable of manufactured home construction. An effort was made to select construction characteristics representative of current construction practice.

The house simulated in this study was a double-wide manufactured house having a floor area of 130.3 m^2 (1402 ft^2) and a 2.44 m (8 ft) ceiling height. The size of the house was based on a control group of 29 manufactured houses studied by Palmiter, Bond, Brown, and Baylon (1992).

A cross section of the roof construction is shown in Figure 3. The sloping roofs faced north and south; the gable end walls faced east and west. The slope of the roof was 14°. The roof construction was comprised of 12 mm (15/32 in.) exterior-grade plywood, asphalt roofing paper, and asphalt shingles. The shingles were medium-dark colored and had a solar absorptance of 0.8. The gable end walls were constructed of 9.5 mm (3/8 in.) asphalt-impregnated fiberboard and vinyl siding. The ceiling construction (or floor of the roof cavity) consisted of 180 mm (7.1 in.) [R-3.9 $m^2 \cdot K/W$ (R-22 $h \cdot ft^{2} \cdot °F/Btu$)] glass-fiber insulation, 0.15 mm (6 mil) kraft paper vapor retarder, and 13 mm (0.5 in.) gypsum board with 575 $ng/s \cdot m^2 \cdot Pa$ (10.0 perm) latex paint applied to its interior surface.

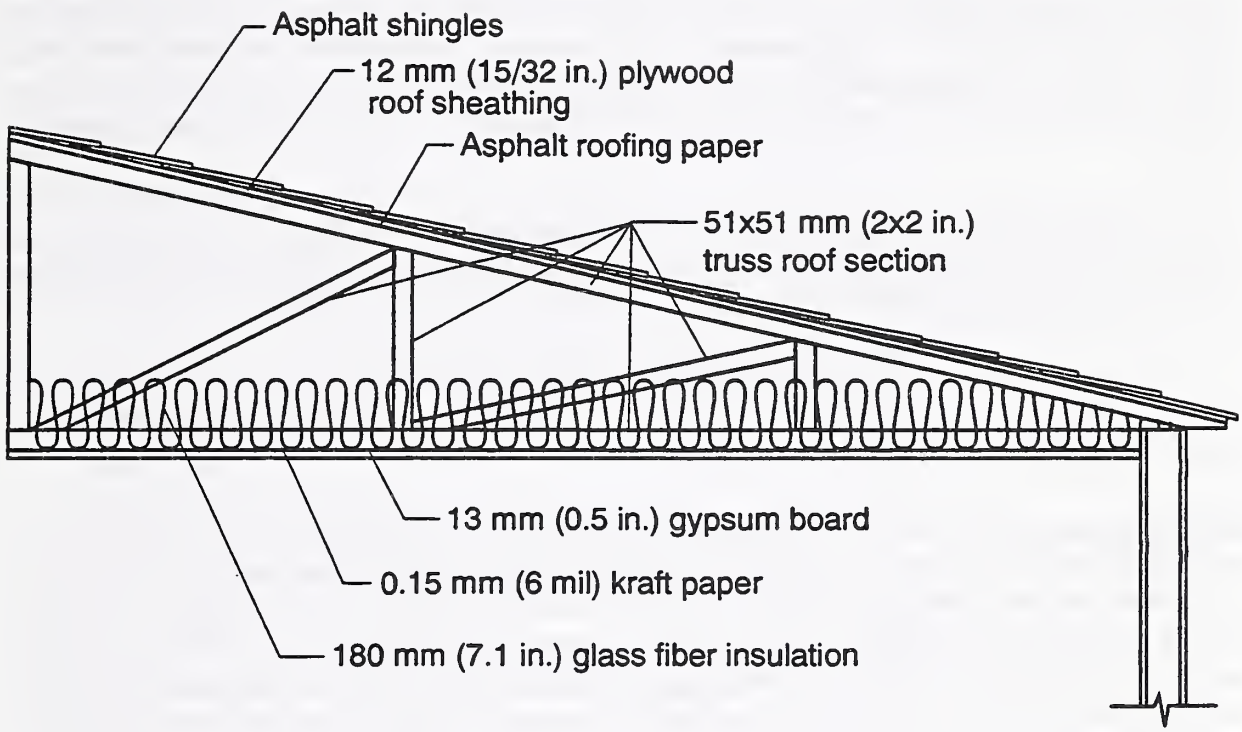

Fig. 3. Half cross-section of roof cavity of double-wide manufactured house.

In the roof and ceiling construction, the framing members (including trusses) were spaced 0.41 m (16 in.) on center.

Based on the control group of 29 houses studied by Palmiter, Bond, Brown, and Baylon (1992), the whole house was assumed to have an effective leakage area (ELA) of 594 cm^2 (92 $in.^2$).[2] Based on airtightness test results of twenty site-built houses (Buchan, Lawton, Parent Ltd 1991), the authors assumed that the ceiling ELA was 35% of the whole house total or 206 cm^2 (32 $in.^2$). The ELA for the house below (excluding the ceiling and roof construction) was 65% of the whole house total or 387 cm^2 (60 $in.^2$).

Consistent with the current HUD Standards for manufactured housing, the gable end walls and the roof construction were fitted with roof cavity vents having a net free open area of 1/300 of the floor area or 4,340 cm^2 (673 $in.^2$). When computer simulations were conducted in a current practice house without roof cavity vents, the authors assumed that unintentional air leakage sites in the construction provided a leakage area of one-tenth that provided by the roof cavity vents themselves or 434 cm^2 (67.3 $in.^2$).

Consistent with the HUD Standards, the current practice house was provided with indoor mechanical ventilation having an average air change rate of 0.00018 m^3/s per m^2 (0.035 ft^3/min per ft^2) of floor area or 0.023 m^3/s (49 ft^3/min).

PARAMETERS USED IN ANALYSIS

Water Vapor Diffusion Properties

Sorption Isotherms. For most of the hygroscopic materials comprising the roof construction of the current practice house, sorption isotherms were measured in the laboratory at the National Institute of Standards and Technology. A sorption isotherm is the relationship between moisture content and relative humidity at equilibrium. The sorption isotherms were determined by placing eight small specimens of each material in vessels above saturated salt-in-water solutions. Each saturated salt-in-water solution provided a fixed relative humidity (Greenspan 1977). The vessels were maintained at a temperature of 24 °C ± 0.2 °C (75 °F ± 0.4 °F) until the specimens reached a steady-state equilibrium. The equilibrium moisture content was plotted versus relative humidity to give the sorption isotherm. Separate sorption isotherm data were obtained for specimens initially dry (adsorption isotherm) and for specimens initially saturated (desorption isotherm). A detailed description of the measurement method is given in Richards et al. (1992).

Edwards (1996) and Hedlin (1967) have studied the effect of temperature on the sorption isotherm for a few building materials and found the effect to be small. For the present analysis, the effect of

---

[2] Under a temperature difference of 16.7 °C (30.0 °F) and a 4.9 m/s (11 mph) wind speed, a house ELA=594 cm^2 (92 $in.^2$) provides a natural house infiltration rate of approximately 0.48 air changes per hour (based on Equation 17).

temperature on the sorption isotherm was neglected.

The mean of the adsorption and desorption isotherm measurements was fit to an equation of the following form:

$$\gamma = \frac{B_1 \phi}{(1+B_2\phi)(1-B_3\phi)} \qquad (19)$$

The coefficients B_1, B_2, and B_3 were determined by regression analysis and are summarized in Table 2. A plot of the sorption isotherms of the materials is given in Figure 4. The asphalt roof shingles and vinyl siding were treated as vapor impermeable materials, and the storage of moisture in these materials was neglected.

The uncertainty in the sorption isotherm measurements was within ± 1.5% moisture content.

Table 2. Sorption Isotherm Regression Coefficients

Materials	B_1	B_2	B_3
Exterior-Grade Plywood Sheathing	0.344	6.18	0.828
Sugar Pine Framing and Truss Members	0.192	2.05	0.765
Glass-Fiber Insulation	0.001703	0.0	0.963
Kraft Paper	51.9	2538.	.902
Gypsum Board	0.00336	0.0	.901
Asphalt-Impreg. Fiberboard	1.14	50.6	0.923
Asphalt Roofing Paper[1]	51.9	2538.	0.902

[1] The regression coefficients for asphalt roofing paper were assumed to be the same as for kraft paper. Since this material is very thin, moisture storage in this material will have very little effect on the predicted moisture content of the plywood roof sheathing. Therefore, the assumed property value may be used in the analysis.

Permeability Measurements. The water-vapor permeability of most of the hygroscopic materials was measured using permeability cups placed in controlled environments. Five circular specimens, 140 mm (5.5 in.) in diameter, of each material were sealed at the top of open-mouth glass cups. The cups were subsequently placed inside sealed glass vessels maintained at a constant temperature. Saturated

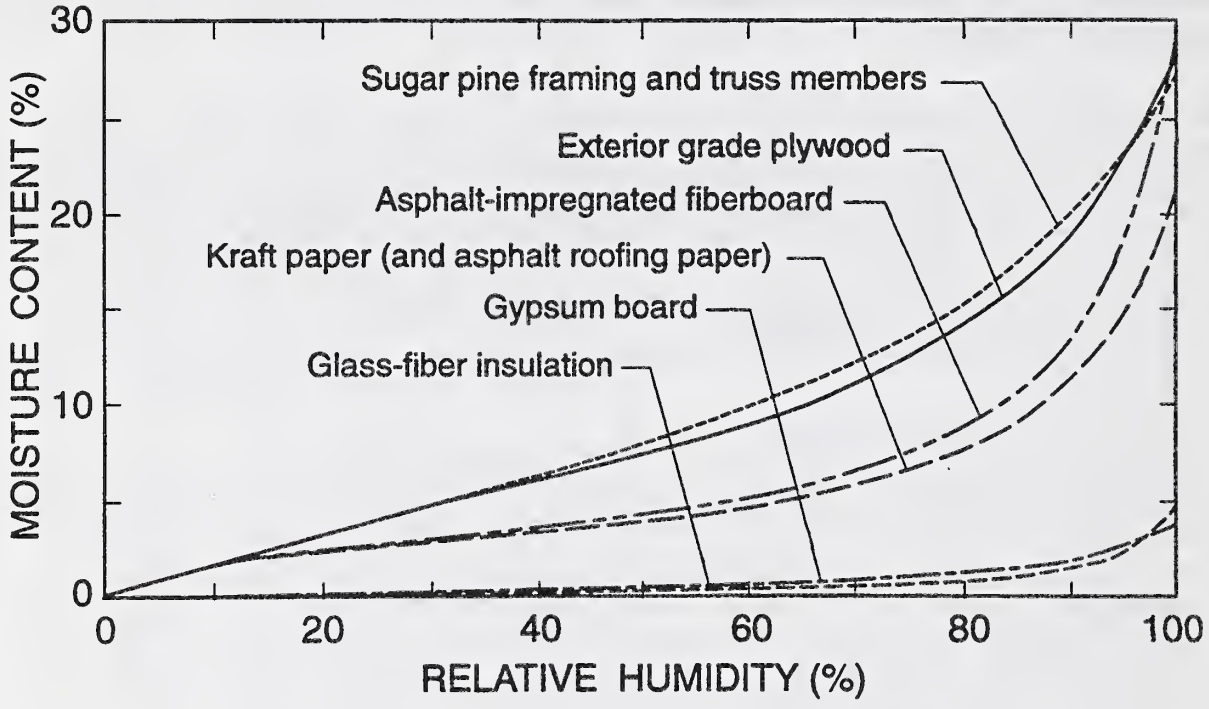

Fig. 4. Sorption isotherms of the materials.

salt-in-water solutions were used inside the glass cups and surrounding glass vessels to generate a relative humidity difference of approximately 10% across each specimen. By using different salt solutions, the mean relative humidities across the specimens were varied over the humidity range of 11% to 97%. Permeability was plotted versus the mean relative humidity across the specimens. Separate measurements conducted at 7 °C (45 °F) and 24 °C (75 °F) revealed that temperature has a small effect on permeability over this particular temperature range. A detailed description of the permeability measurement method is given in Burch et al. (1992).

Water vapor permeability data were plotted versus the mean relative humidity across the specimen and fit to an equation of the form:

$$\mu = C_1 + C_2 \exp(C_3 \phi) \tag{20}$$

Here the permeability (μ) is expressed in ng/s·m·Pa. The coefficients C_1, C_2, and C_3 were determined by regression analysis and are summarized in Table 3. A plot of the permeance (i.e., permeability divided by thickness) of the materials is given in Figure 5. The asphalt roof shingles and vinyl siding were treated as vapor impermeable materials.

The uncertainty in measuring the permeability of the materials was less than 5% when measuring materials having a permeance less than 575 ng/s·m^2·Pa (10 perm). However, the uncertainty increased rapidly as the specimen permeance rose above 575 ng/s·m^2·Pa (10 perm).

The mass transfer coefficients for the boundary air layers in contact with surfaces of the roof cavity were predicted using the Lewis relationship between heat and mass transfer (Threlkeld 1970). The permeance of the latex paint was assumed to be 575 ng/s· m^2·Pa (10 perms).

Liquid Diffusivity

In a few of the simulations, the moisture content in the plywood roof sheathing and the wood framing members rose above fiber saturation during the winter. Liquid water coalesced within the "large" pores of the materials. Under this condition, capillary transfer occurred, and liquid diffusivity is the fundamental moisture transport coefficient. The hydraulic conductivity (K) in Equation (1) is related to the liquid diffusivity (D_γ) by the relation:

$$K = -\frac{\rho_d D_\gamma}{\frac{\partial p_l}{\partial \gamma}} \tag{21}$$

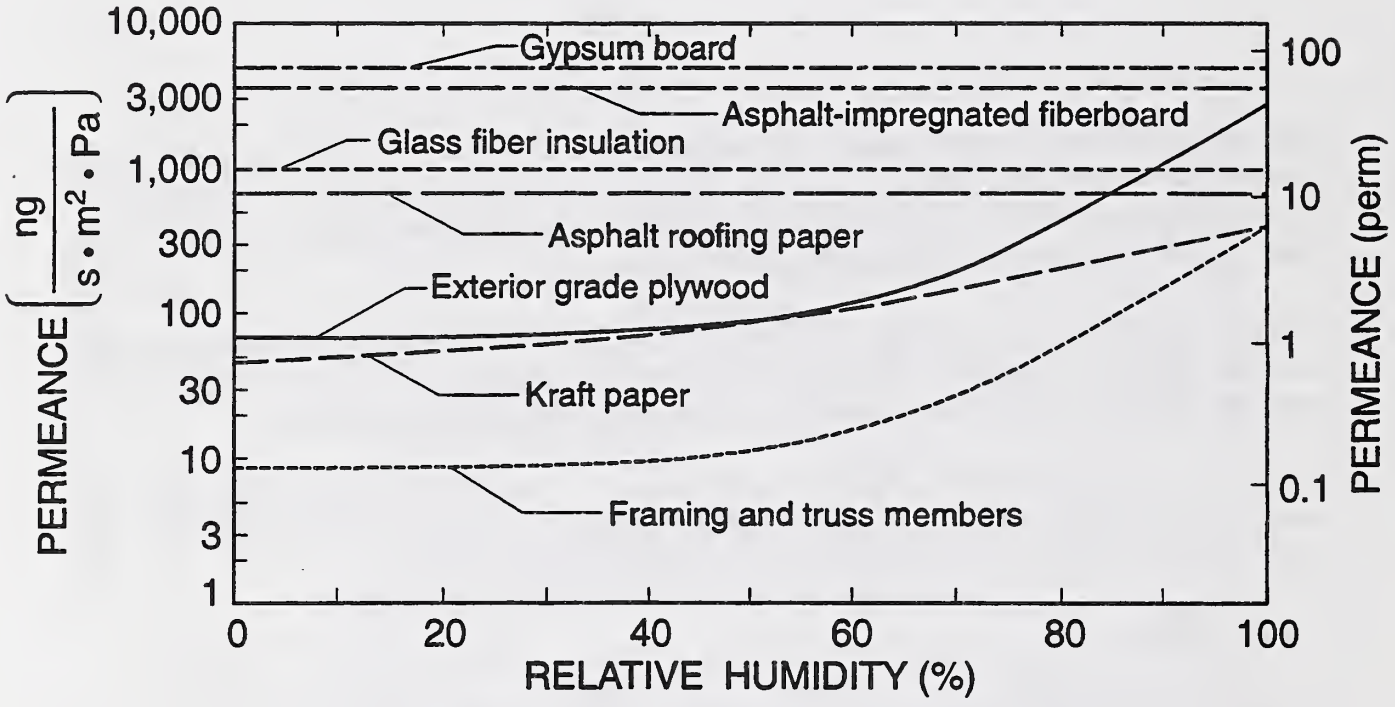

Fig. 5. Water vapor permeances of materials.

Table 3. Permeability Regression Coefficients			
Materials	C_1	C_2	C_3
Exterior-Grade Plywood Sheathing	0.806	0.00163	9.765
Sugar Pine Framing and Truss Members	0.442	0.000910	9.86
Glass-Fiber Insulation[1]	182	0.0	0.0
Kraft Paper	0.00626	0.000896	4.01
Gypsum Board	63.8	0.0	0.0
Asphalt-Impreg. Fiberboard	34.4	0.0	0.0
Asphalt Roofing Paper[2]	0.511	0.0.	0.0

[1] The permeability of glass-fiber insulation was assumed to be equal to the permeability of a stagnant air layer. This assumption is reasonable because the glass fibers of the insulation occupy a small fraction of its volume. Bound-water diffusion along the glass fibers is small compared with molecular diffusion through the predominantly open pore space.

[2] Based on data contained in ASHRAE (1993).

where the term in the dominator of the right side of the equation is the derivative of the capillary pressure with respect to moisture content.

For the plywood roof sheathing, the authors used liquid diffusivity measurements for grooved exterior-grade plywood (Richards 1992). For the framing members, the authors used liquid diffusivity measurements for sugar pine (Richards 1992). The authors believe that they were justified in using liquid diffusivity measurements of similar materials for the following reasons. In most of the computer simulations, the materials operated entirely in the hygroscopic regime and the capillary coefficients were never used in the calculations. In the remainder of the computer simulations, the material operated predominantly in the hygroscopic regime and moved into the capillary regime only during brief periods, except for two worst case houses (i.e., very high indoor relative humidity without attic ventilation). Moreover, the capillary transfer coefficient does not govern how much moisture reaches the plywood layer, but rather the re-distribution of moisture across the thickness of the plywood layer. Very little liquid water is transferred to the adjacent building paper because the building paper offers high resistance to capillary flow.

Airflows

Roof Cavity Ventilation Rate. Buchan, Lawton, Parent Ltd (1991) measured sixty attic ventilation rates in twenty houses in several Canadian climates. The houses had different types of attic ventilation with a wide range of ELA's measured using a pressurization technique. For each of the measurements, they also measured the wind speed, wind direction, and temperature difference between the roof cavity and the outdoor environment. The authors applied Equation 8 to this set of data and used regression analysis to determine the empirical coefficients. The stack coefficient ($C_{\Delta T,c}$) was determined to be a very small value and was taken to be zero. The wind coefficient ($C_{V,c}$) was found to be 6.94 x 10^{-5} $(L/s)^2 \cdot (cm)^{-4} \cdot (m/s)^{-2}$ [0.00259 $cfm^2 \cdot in.^{-4} \cdot mph^{-2}$].

A plot of the volumetric attic ventilation rate per unit roof effective leakage area as a function of wind speed is given in Figure 6. Each point represents one of the measurements of Buchan, Lawton, Parent Ltd (1991). The least-squares-fit correlation is also given in the plot of Figure 6. It should be noted that a great deal of scatter exists between the least-squares-fit correlation and the measurement points. A contributing factor is that the least-squares-fit correlation does not include wind direction and attic ventilation type. Upper and lower bounds for the measured data are also shown on the plot. With the exception of a few points deemed to be outliers, most of individual measurements fall between the upper and lower bounds.

House Natural Ventilation Rate. For the semi-empirical relation (Equation 17), the stack coefficient ($C_{\Delta T,h}$) was taken to be the ASHRAE (1993) value 0.000145 $(L/s)^2 \cdot cm^{-4} \cdot °C^{-1}$ [0.0156 $cfm^2 \cdot in.^{-4} \cdot °F^{-1}$] for a one-story house. The wind speed coefficient ($C_{V,h}$) was taken to be the ASHRAE (1993) value 0.000104 $(L/s)^2 \cdot (cm)^{-4} \cdot (m/s)^{-2}$ [0.0039 $cfm^2 \cdot in.^{-4} \cdot mph^{-2}$] for a one-story house with a shielding class of 4.

Heat

The thermal conductivity, density, and specific heat of the materials were taken from ASHRAE (1993).

Other Properties

The long-wave emittance of the materials was taken to be 0.9. The solar absorptances of the asphalt roofing shingles and the vinyl siding applied to the gable end walls were taken to be 0.8 and 0.6, respectively. The 0.8 absorptivity value is the mean value measured by Parker, et al. (1993) for thirty-four different colored asphalt roof shingles.

Indoor and Outdoor Conditions

In the computer analysis, the hourly outdoor boundary conditions (i.e., ambient temperature, relative humidity, wind speed, and incident solar radiation) were obtained from ASHRAE WYEC weather data (Crow 1981). During the winter when space heating was required, the set point temperature was

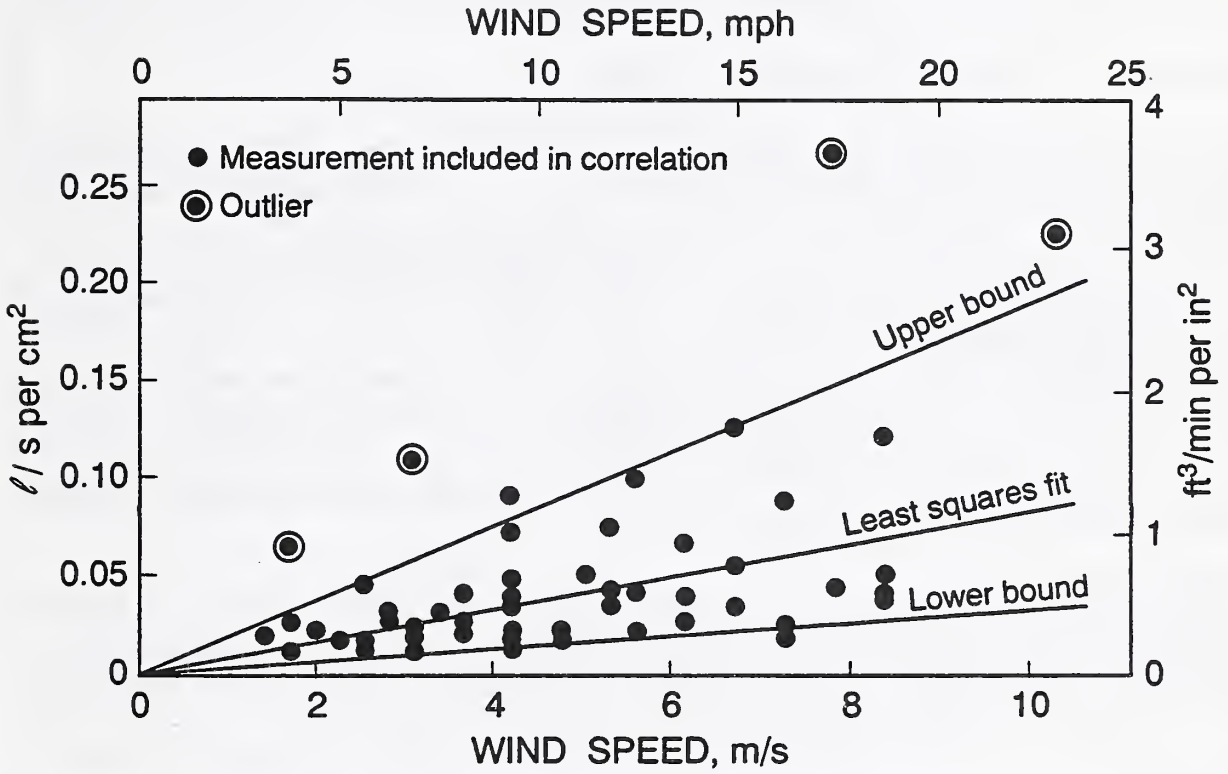

Fig. 6. Volumetric attic ventilation rate per unit roof effective leakage area plotted as a function of wind speed [measurements taken from Buchan, Lawton, Parent Ltd (1991)].

20 °C (68 °F). The occupant activities produced moisture at a rate of 10.9 kg/day (24.0 lb/day) unless stated otherwise, and the indoor relative humidity during the winter was predicted from a moisture balance of the whole building. During the summer when space cooling was required, the set point temperature and indoor relative humidity were 24 °C (76 °F) and 56%, respectively.

Six months of weather data were used to initialize the reported one-year simulation results in order to reduce the effect of assumed initial construction layer moisture content and temperature. The moisture performance of the prototype roof was analyzed for the cold climates of Madison, WI (most simulations); Boston, MA; Portland, OR; and Atlanta, GA; as well as the hot and humid climate of Miami, FL.

COLD CLIMATE RESULTS

Performance of Current-Practice House in Madison

The new attic model was first used to predict the weekly average moisture content of the roof cavity surfaces for the current-practice house located in Madison, WI. The surface moisture contents are plotted versus time of year in Figure 7. The moisture content of the roof rafters (not shown) tended to track the plywood roof sheathing but were slightly lower. The surface moisture contents are lowest during summer and rise to a maximum during fall and winter. The construction component having the highest surface moisture content is the north sloping plywood roof. The peak plywood moisture content is seen to be 16% (dry mass basis), and is well below fiber saturation (i.e., a moisture content of 28%). It should be pointed out that the moisture control practices (i.e., installing an interior ceiling vapor retarder and providing passive roof cavity vents consistent with the 1/300 rule) are implemented on this house. The volumetric attic ventilation rate was predicted using the least-squares-fit correlation (see Figure 6).

The model was next used to investigate the relative importance of various parameters on the roof cavity performance. The approach was to vary one parameter at a time and investigate its effect on the moisture content of the north sloping plywood roof. Henceforth in this report, the winter analysis will focus on the moisture content of the north sloping plywood roof, since this construction component always had the highest moisture content. Unless stated otherwise, the climate is Madison, WI.

Effect of Roof Cavity Ventilation

Passive Roof Cavity Ventilation. The model was next used to investigate the consequences of not providing any roof cavity vents. When the ventilation openings were not present, it was assumed that unintentional air leakage sites in other parts of the construction provided an ELA of 434 cm^2 (67.3 $in.^2$) which was one-tenth of that provided by the passive ventilation openings themselves. Figure 8 compares the north sloping roof moisture content of two identical current-practice houses, one with and the other without roof cavity vents. When roof cavity vents were provided, their ELA was set equal to the net free open area specified by the 1/300 rule. In the house without roof cavity

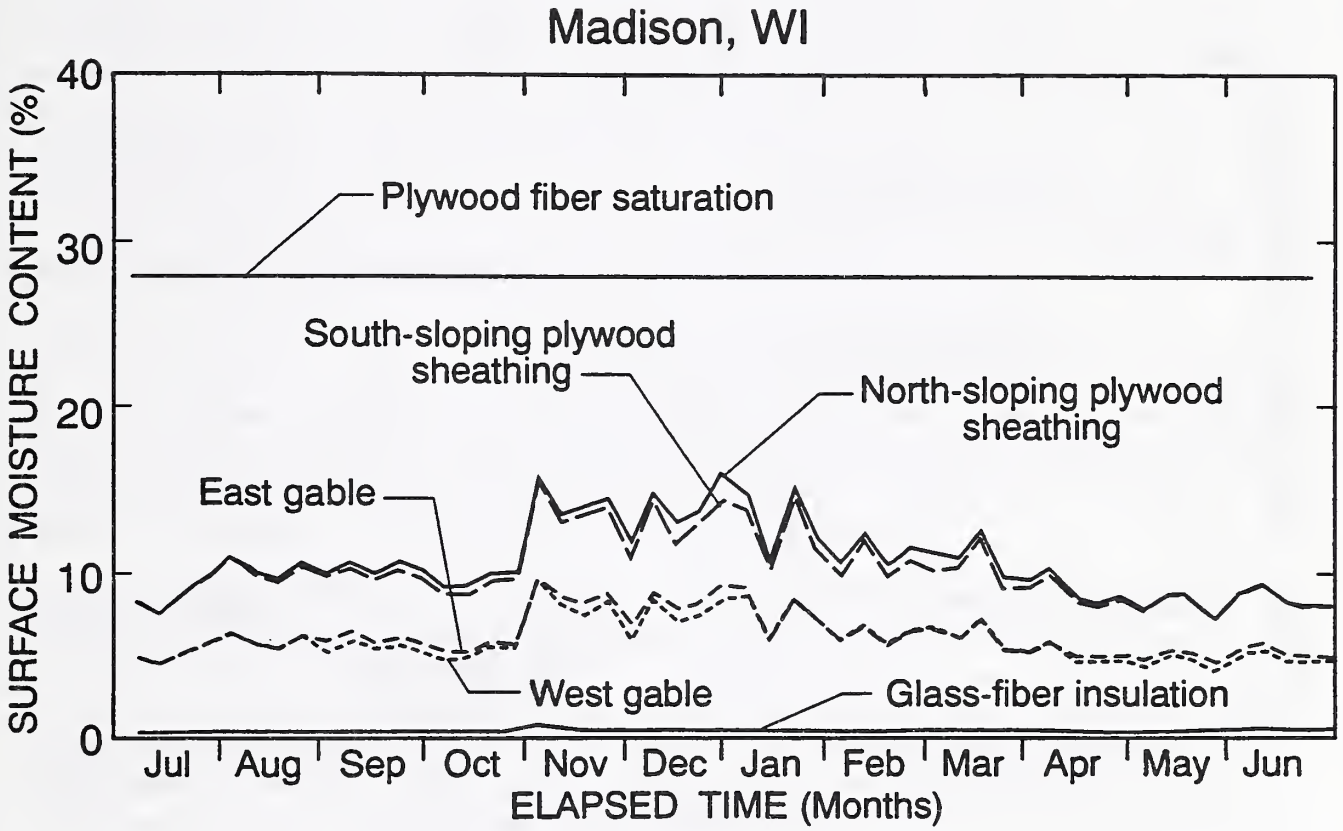

Fig. 7. Surface moisture content of roof cavity construction materials for the current practice house.

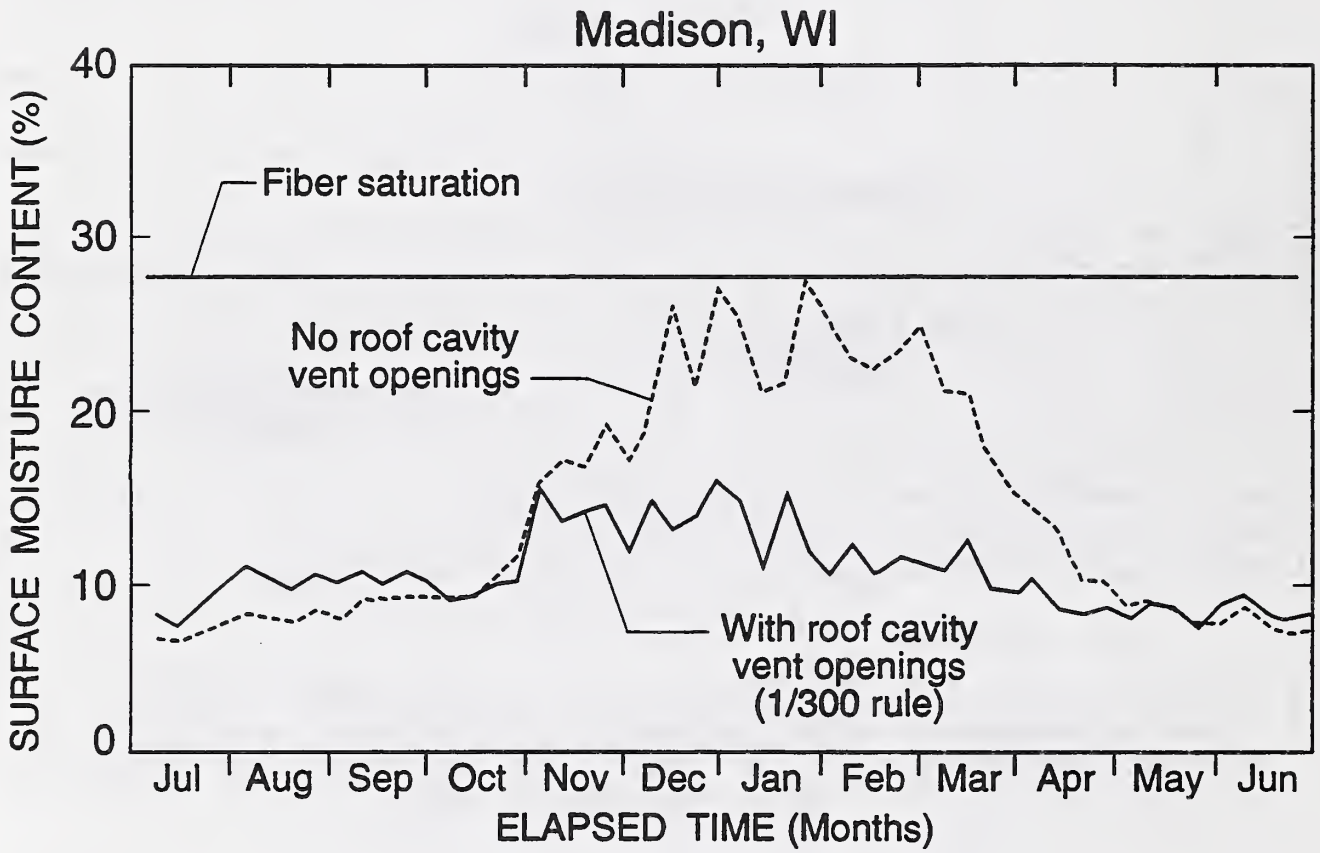

Fig. 8. Effect of passive roof cavity ventilation on the moisture content of north-sloping plywood roof sheathing for current practice house.

vents (upper curve), the moisture content rises almost to fiber saturation (depicted by the horizontal line at 28% moisture content). On the other hand, in the house with roof cavity vents (lower curve), the moisture content is maintained well below fiber saturation. These results demonstrate that appropriately sized roof cavity vents are very effective in removing moisture and maintaining the roof sheathing moisture content at acceptable levels.

Mechanical Roof Cavity Ventilation. The model was next used to investigate the effectiveness of the specified mechanical ventilation rate in the HUD Standards that permits mechanical ventilation to be substituted for passive roof cavity vents. The HUD Standards specify that the mechanical ventilation rate shall be at least 0.00010 m^3/s per m^2 (0.02 ft^3/min per ft^2) of attic floor. The current practice house has a floor area of 130 m^2 (1402 ft^2), and the mechanical ventilation rate is calculated to be 0.013 m^3/s (28 ft^3/min). The results of a computer simulation with the roof cavity ventilated at this constant rate are shown in Figure 9. Note that the predicted moisture content of the plywood roof sheathing (upper curve) rises to fiber saturation during the winter. These results indicate that the mechanical attic ventilation rate specified in the HUD Standards is too low under some conditions and needs to be increased to achieve acceptable performance. This is especially critical since some houses will have greater moisture flow into the attic than assumed in this analysis.

The previous results with passive roof cavity vents provided satisfactory performance (see Figure 8). An effort was made to find a mechanical ventilation rate that would provide the same amount of attic ventilation as the passive ventilation openings operated under prevailing outdoor wind speeds. From the *Climatic Atlas of the United States* (1983), the mean January wind speed for many parts of the United States is approximately 4.9 m/s (11 mph). From Equation 8, an equivalent mechanical ventilation rate of 0.175 m^3/s (370 ft^3/min) was determined.

A computer simulation was carried out using the above equivalent mechanical ventilation rate of 0.175 m^3/s (370 ft^3/min). In addition, simulations were conducted at attic mechanical ventilation rates of 0.123 m^3/s (260 ft^3/min) and 0.068 m^3/s (144 ft^3/min). The results are included in Figure 9. Notice that all of the above revised mechanical ventilation rates had roof sheathing moisture contents that were well below fiber saturation. Based on these results, it is recommended that the prescribed mechanical attic ventilation rate be the lower of the revised rates or 0.068 m^3/s (144 ft^3/min). Expressing this figure on a per unit attic floor area, the specified mechanical attic ventilation rate should be 0.0005 m^3/s per m^2 (0.1 ft^3/min per ft^2).

Effect of a Ceiling Vapor Retarder

The model was next used to investigate the effect of a ceiling vapor retarder. Separate computer simulations were carried out with and without a ceiling vapor retarder. The results are given in Figure 10a for a house with roof cavity vents and in Figure 10b for a house without roof cavity vents. The presence of the vapor retarder has a small effect on the roof sheathing moisture content. This is because water vapor diffusion is transporting much less moisture than airflow from the house into the roof cavity as shown in the next section. A ceiling vapor retarder had a small effect because airflow from the house into the roof cavity was the dominant moisture transport mechanism.

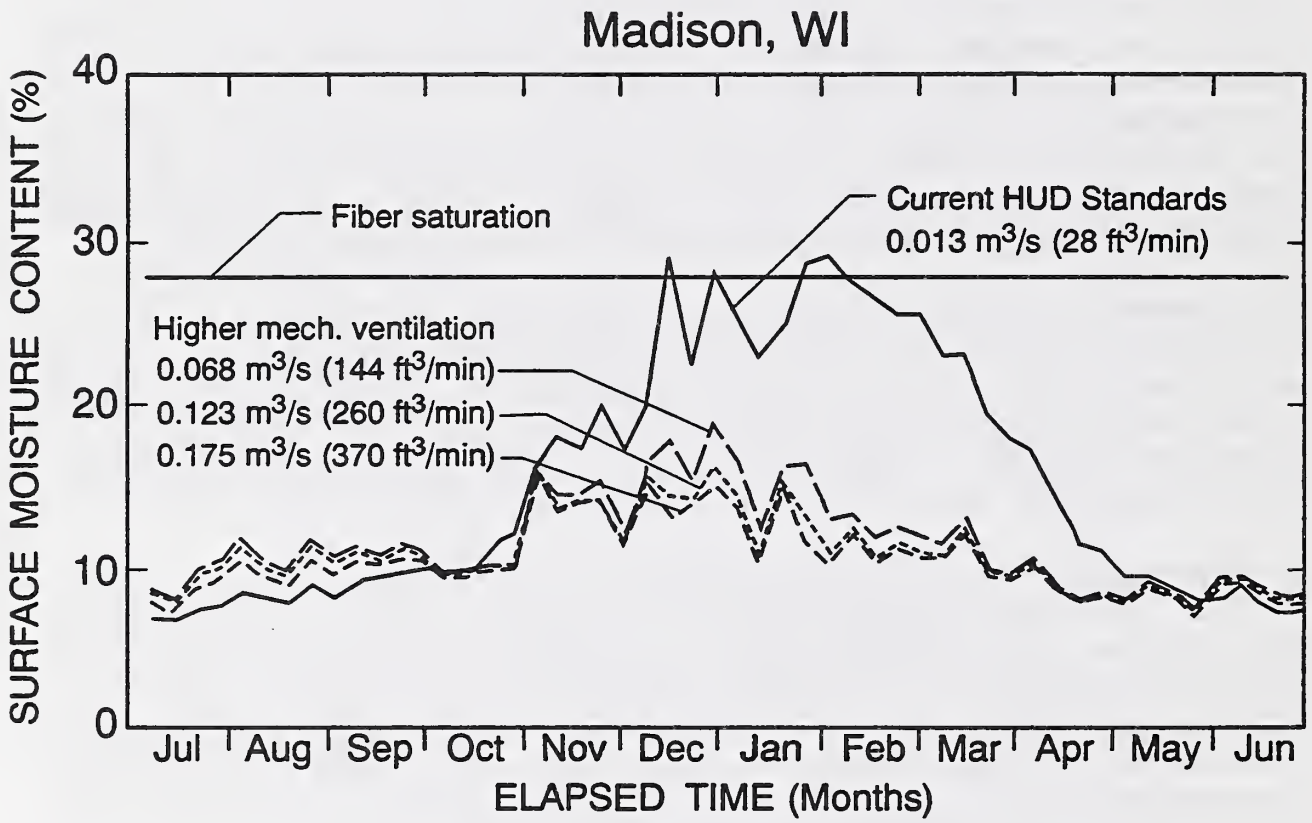

Fig. 9. Effect of mechanical roof cavity ventilation on the moisture content of north-sloping plywood roof sheathing for current practice house.

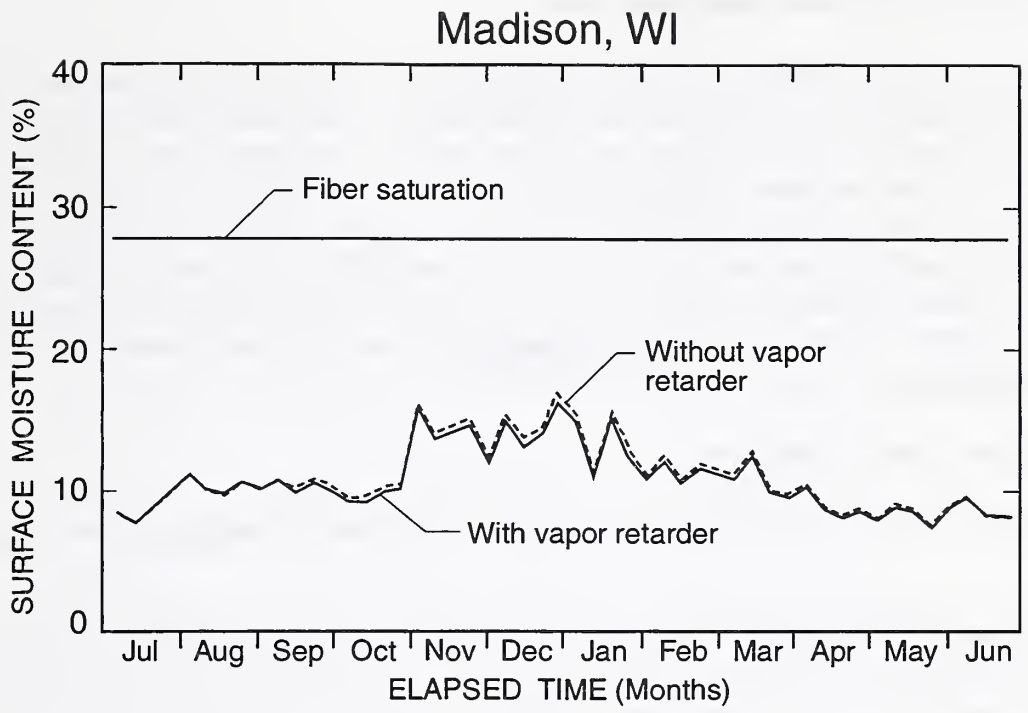

a. With passive attic ventilation (1/300 rule)

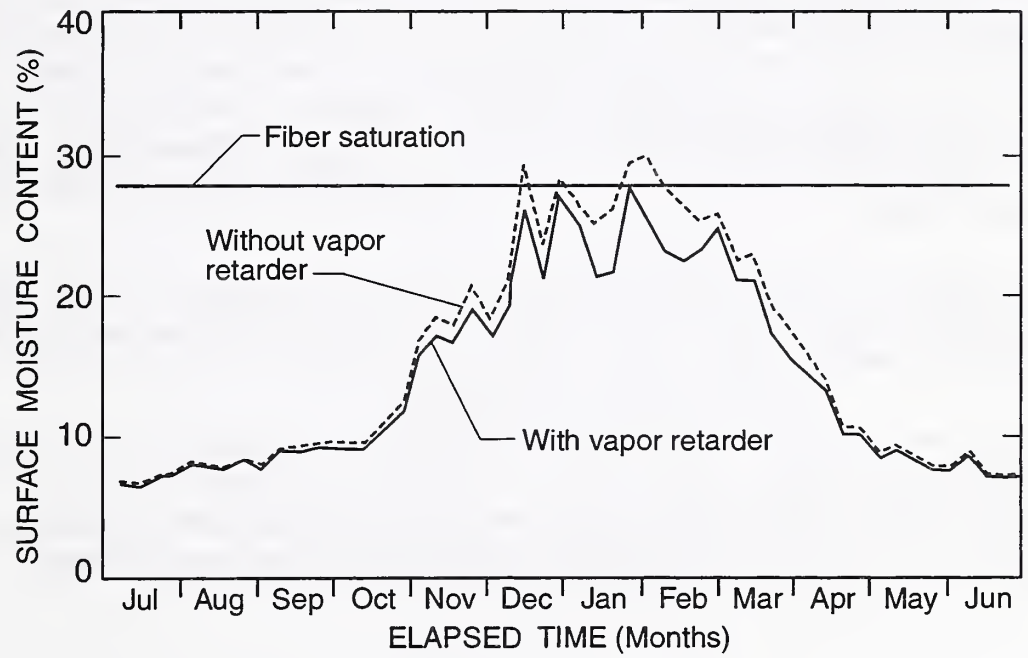

b. Without passive attic ventilation (1/300 rule)

Fig. 10. Effect of an interior ceiling vapor retarder on the moisture content of north-sloping plywood roof sheathing for current practice house.

Effect of Airflow from House into Roof Cavity

A simulation was next conducted of the current practice house with the ceiling ELA reduced to zero, thereby eliminating airflow from the house into the roof cavity. The current practice house without airflow (lower curve) is compared to the same house with a representative airflow in Figure 11. Representative airflow was achieved by using a wall ELA of 387 cm^2 (60 in^2), a ceiling ELA of 206 cm^2 (32 in^2), and a roof ELA of 4,340 cm^2 (673 in^2) in the stack-effect airflow equations. Here the roof ELA is set equal to the net free opening specified by the 1/300 rule.[3] When the ceiling airflow is zero, the roof sheathing moisture content is lower. Comparing these results to the previous results of Figure 10, airflow is seen to have a larger impact on the roof sheathing moisture content than water vapor diffusion.

Effect of Indoor Relative Humidity

In this section, the effect of indoor relative humidity on the roof sheathing moisture content is analyzed.

Humidified Houses. The current practice house was simulated with a humidifier that maintained a constant indoor relative humidity of 45% during the winter. An indoor relative humidity of 45% is the highest humidity that can be maintained without condensation on double-pane windows. The roof sheathing moisture content of the humidified house is compared to the same house without humidification in Figure 12a. In the humidified house (upper curve), the moisture content of the north sloping plywood roof sheathing rose to a peak of 25% and approached fiber saturation (28%). Note, however, that both roofs dry out quickly in the spring. Here the rate of moisture transport from the house into the roof cavity is approaching the limit of effective removal by passive attic ventilation. The large difference in roof sheathing moisture content between the humidified and non-humidified house is a direct consequence of the indoor relative humidity difference between the two houses depicted in Figure 12b.

Non-Humidified Houses. A number of factors affect the indoor relative humidity in non-humidified houses, including the indoor moisture production rate, the house ELA, and indoor mechanical ventilation, when it is present.

Separate computer simulations of the current practice house were conducted with the following moisture production rates: high: 16.3 kg/day (36 lb/day), typical: 10.9 kg/day (24 lb/day), and low: 5.4 kg/day (12/day). The resulting plywood moisture contents and indoor relative humidities are shown in Figures 13a and 13b, respectively. As the moisture production rate increases, the peak plywood moisture content is seen to rise in response.

---

[3] In a strict sense, effective leakage area is somewhat different than net free area due to airflow entrance effects.

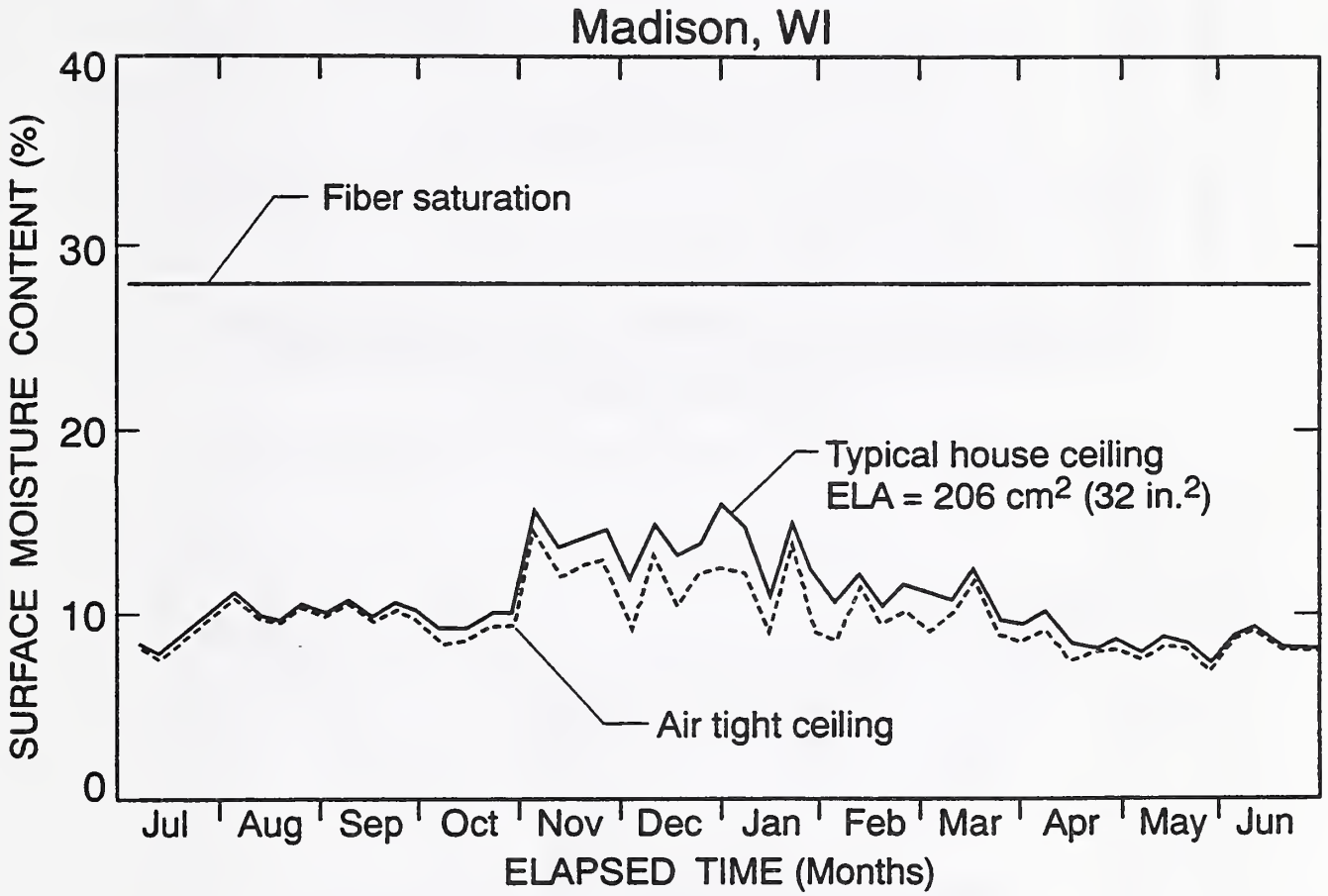

Fig. 11. Effect of airflow from house into roof cavity on the moisture content of north-sloping plywood roof sheathing for current practice house.

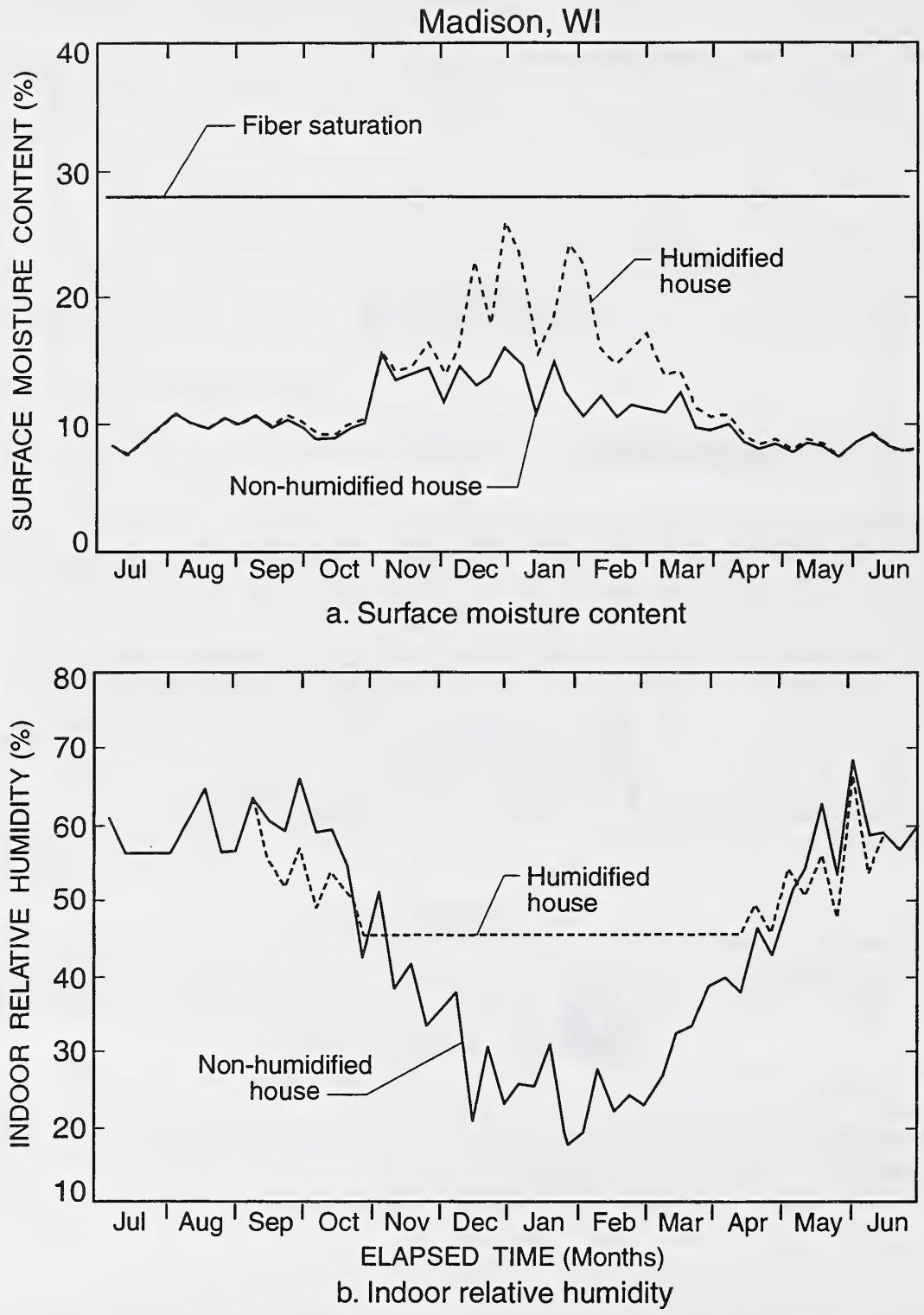

Fig. 12. Effect of indoor humidification on the moisture content of north-sloping plywood roof sheathing and indoor relative humidity for current practice house.

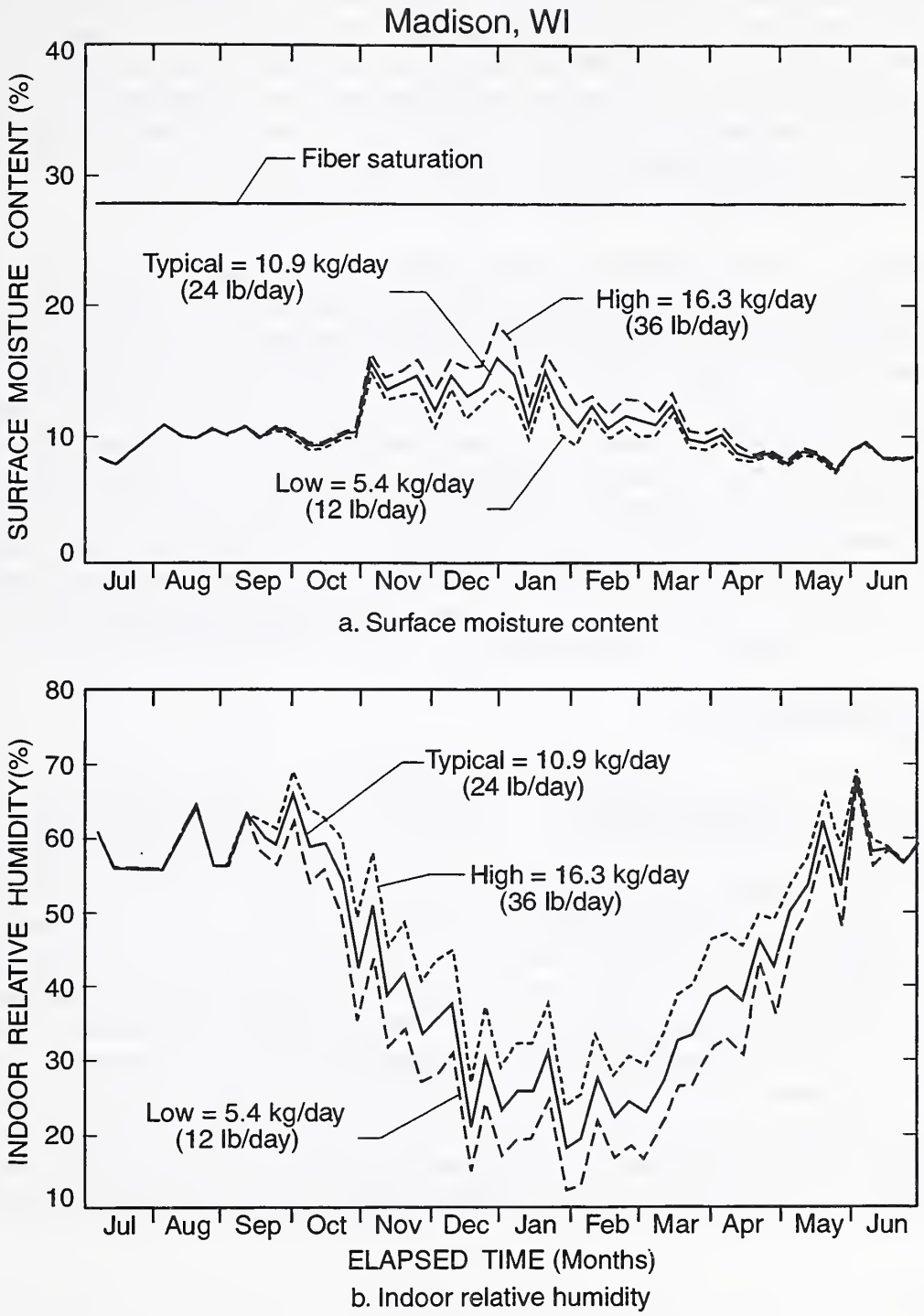

Fig. 13. Effect of moisture production rate on the moisture content of north-sloping plywood roof sheathing and indoor relative humidity for current practice house.

Several simulations of the current practice house were conducted with the following three house ELA's: a leakier house: ELA=787 cm^2 (122 in^2), a typical house: ELA=594 cm^2 (92 in^2), and a tighter house: ELA=400 cm^2 (62 in^2). In these simulations, the ceiling ELA was maintained at a constant value of 206 cm^2 (32 in^2). Here the authors assumed that ceiling air leakage through partition walls, ceiling light fixtures, plumbing and HVAC penetrations would remain constant as the exterior wall ELA was varied. These three simulation are shown in Figure 14. As the house becomes tighter, less natural infiltration occurs, and the indoor relative humidity rises. This causes the roof sheathing moisture content to slightly increase during the fall and winter.

Several simulations were also conducted with the following three levels of continuous indoor mechanical ventilation: none, the current practice house at a typical rate of 0.023 m^3/s (49 ft^3/min), and at a very high rate of 0.071 m^3/s (150 ft^3/min). These ventilation rates are actual values, as opposed to rated values. The high ventilation rate corresponds to continuous operation of the kitchen and bathroom ventilation exhaust fans or a large exhaust only whole house ventilation system. The typical rate is the ventilation rate currently specified by the HUD Standards. Predicted roof sheathing moisture contents for the three cases are given in Figure 15. The results indicate that indoor mechanical ventilation slightly decreases the moisture content of the roof sheathing due to reductions in indoor relative humidity. The results of Figure 15 also indicate that, if the homeowner were to modify the HVAC equipment and turn off the continuous ventilation specified in the HUD Standards, then the roof sheathing moisture content would increase by only approximately 2%, but moisture levels are still below fiber saturation (28%).

Effect of Outdoor Climate

The model was next used to simulate the current practice house in the following four winter climates: a very cold climate (Madison, WI), a moderately cold climate (Boston, MA), a mild climate (Atlanta, GA), and cool Pacific northwest climate (Portland, OR). The roof sheathing moisture content and indoor relative humidity values are depicted in Figure 16a and 16b, respectively. These results show a considerably smaller sensitivity to climate compared with previous results (Burch 1995) in which the indoor relative humidity was maintained constant during the simulation. The present results with variable indoor relative humidity show less climatic sensitivity because the indoor relative humidity is lower in cold climates during the winter months (see Figure 16b). This diminishes the vapor pressure potential for the moisture transport. On the other hand, milder climates tend to have higher indoor relative humidities during winter months, but there is less opportunity for condensation. The small effect of climate on winter moisture accumulation has also been reported to occur in walls when the indoor relative humidity is permitted to vary during the winter rather than being held constant (Tsongas, Burch, Roos, and Cunningham 1995).

Other Factors

The model was used to simulate the current practice house with the following four winter set point temperatures: 17.2 °C (63 °F), 20.0 °C (68° F), 22.8 °C (73 °F), and 25.6 °C (78 °F). The results,

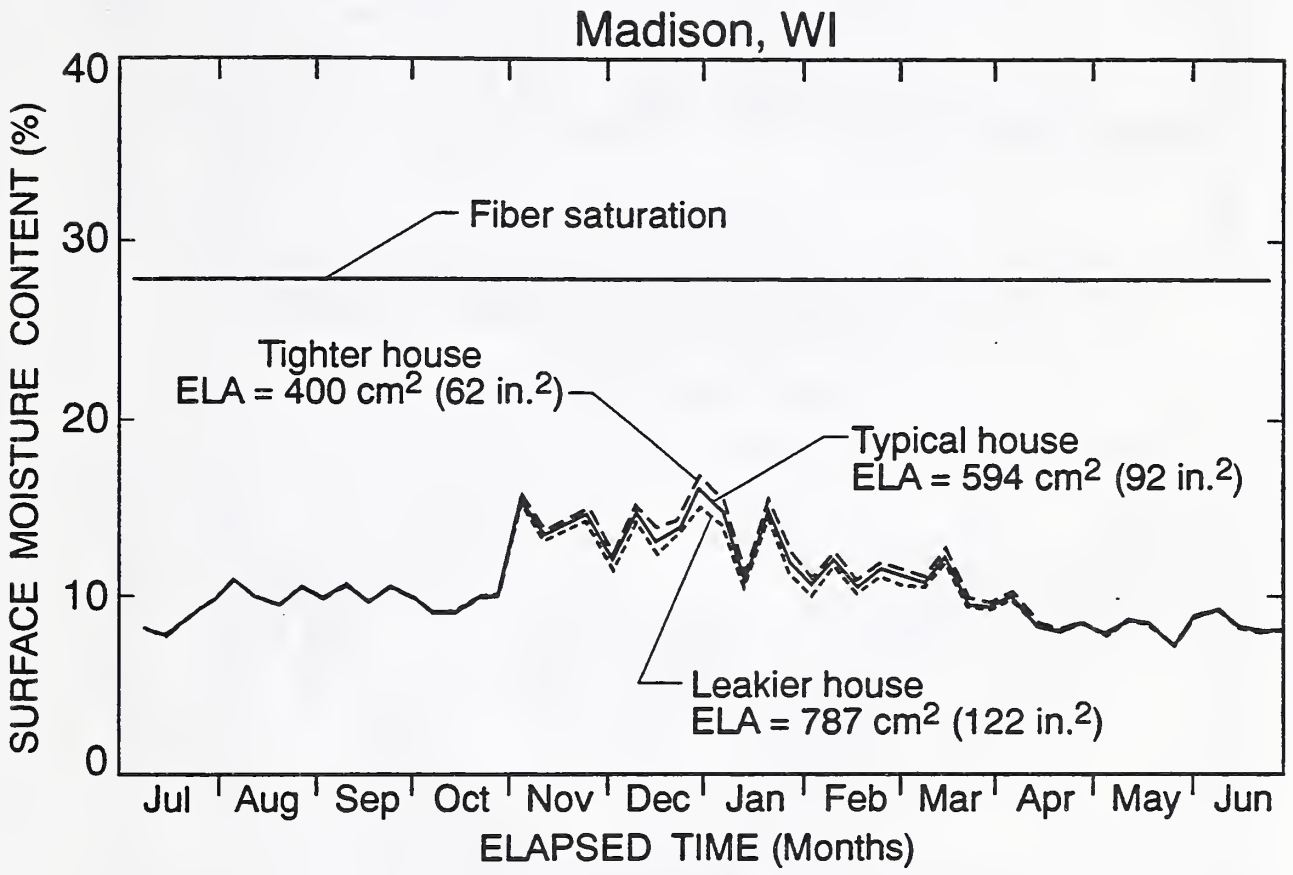

Fig. 14. Effect of house tightness on the moisture content of north-sloping plywood roof sheathing for current practice house.

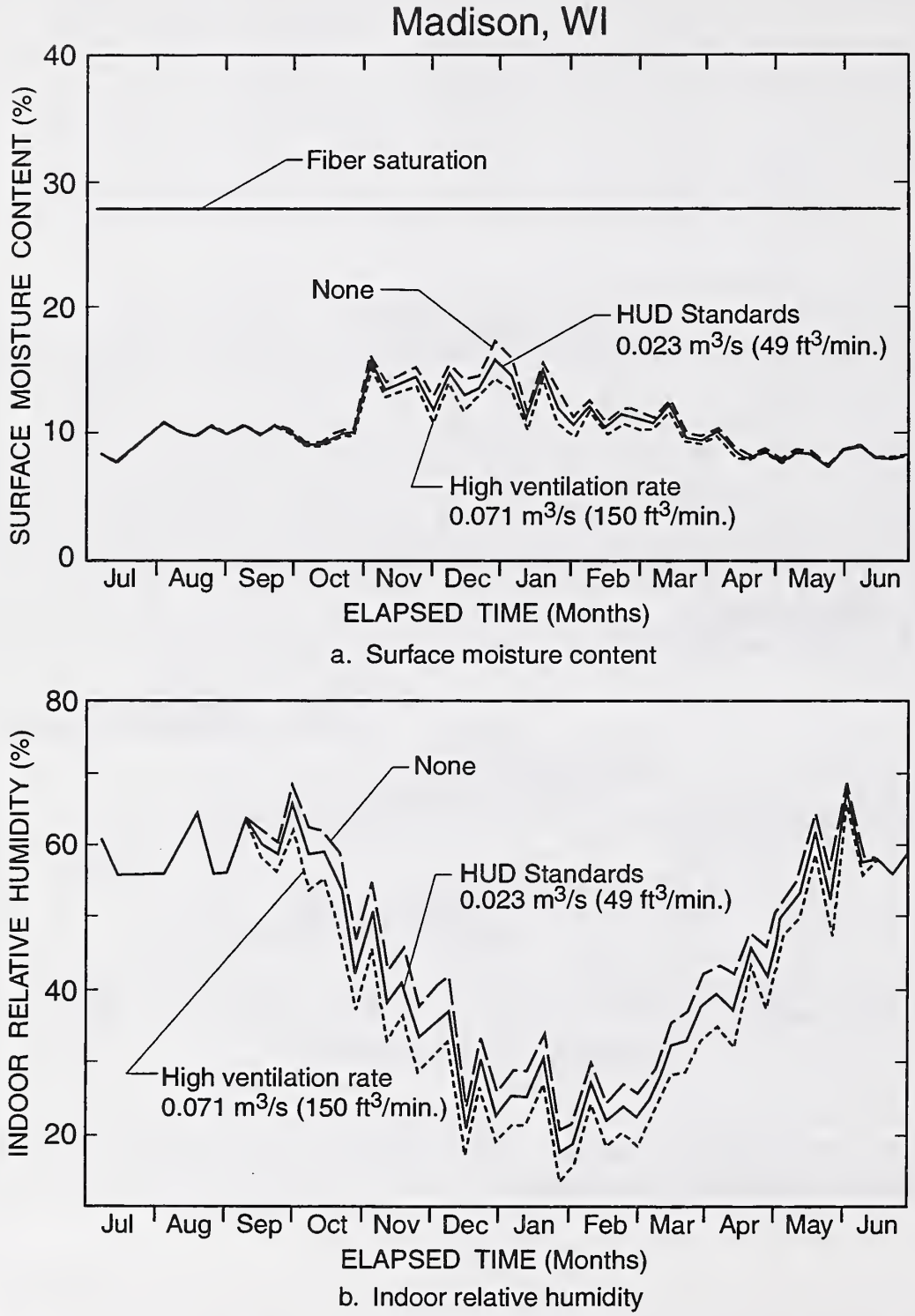

Fig. 15. Effect of indoor mechanical ventilation on the moisture content of north-sloping plywood roof sheathing and indoor relative humidity for current practice house.

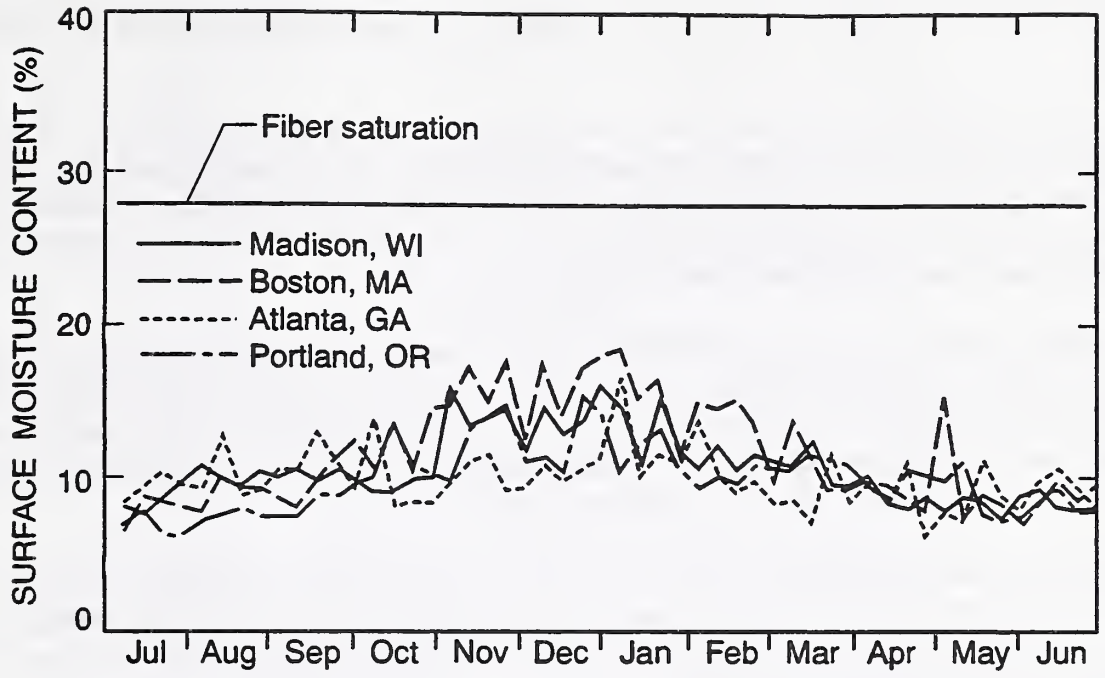

a. Surface moisture content

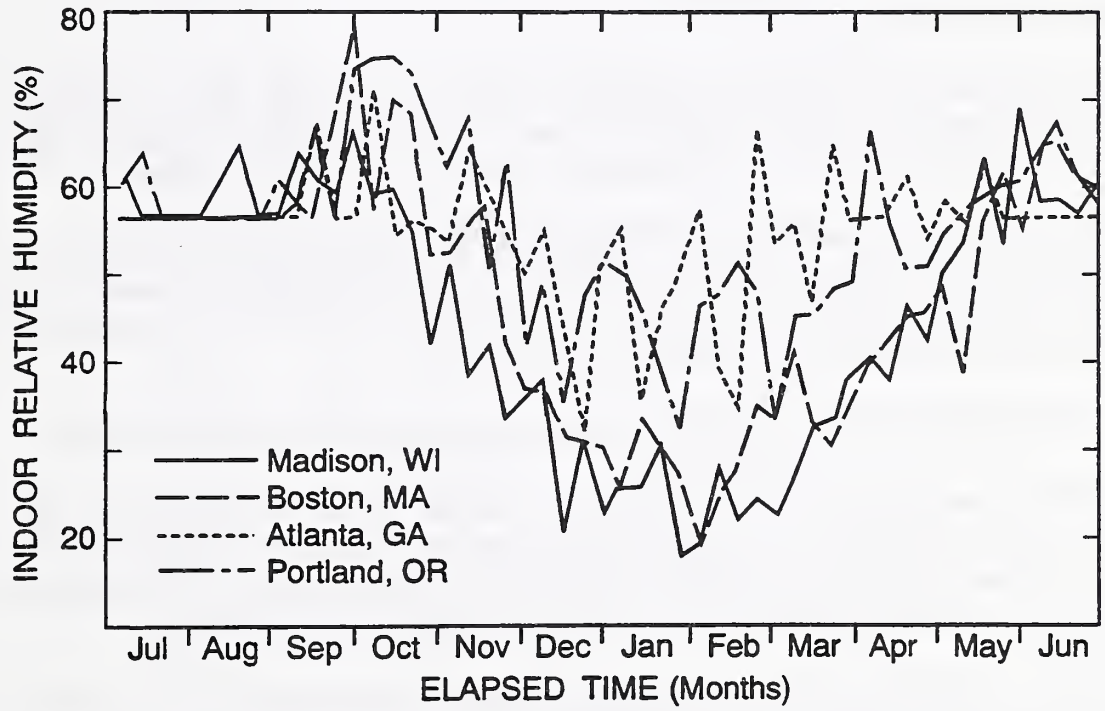

b. Indoor relative humidity

Fig. 16. Effect of outdoor climate on the surface moisture content of north-sloping plywood roof sheathing and indoor relative humidity for current practice house.

plotted in Figure 17a, reveal that slightly more moisture accumulates in the roof sheathing of colder houses.

The current practice house was next simulated with sky radiation turned off in the model. This result is compared to the same house with sky radiation in Figure 17b. This comparison indicates that the roof sheathing moisture content is about 4% mc higher when sky radiation is included in the analysis. This is because thermal radiation to the sky significantly reduces the roof sheathing temperature, and thereby increases the roof sheathing moisture content.

The current practice house was simulated with a light colored roof (solar absorptance = 0.65), a medium colored roof (solar absorptance = 0.8), and a dark colored roof (solar absorptance = 0.95). The results given in Figure 17c reveal that dark colored roofs have a slighter lower roof sheathing moisture content. This is because they absorb more solar energy and operate at a higher temperature and thereby decrease the roof sheathing moisture content.

A simulation of the current practice house was also conducted without the interior wood trusses. When this result was plotted (not shown) and compared to the same house with the interior wood trusses, both results were observed to be almost identical, thereby indicating that wood trusses play an insignificant role in the moisture performance of ventilated roof cavities.

Summary of Effect of Parameters

The effect of the various parameters on the moisture content of the roof sheathing is summarized in Table 4. The difference in moisture content presented in the last column is the maximum estimated difference in moisture content observed at the peak roof sheathing moisture content.

From Table 4, attic ventilation (both passive and mechanical) and indoor humidification are seen to affect the roof sheathing moisture content by more than 12% mc. The effect of outdoor climate, sky temperature, and indoor moisture generation rates are somewhat less, ranging between 4-7% mc. The effects of the other parameters are each less than 3% mc.

PROVIDING WHOLE HOUSE VENTILATION WITH CEILING VENTS

It is possible to provide whole house ventilation by installing several ventilation openings in the ceiling of a manufactured house. Ceiling vents will increase the airflow from the house into the attic and thereby reduce the indoor relative humidity. However, increased airflow will transport more moisture into a roof cavity and increase the space heating load as shown below.

Two computer simulations of the current practice house were conducted with two ceiling vent openings each having an ELA of 310 cm^2 (48 in^2). These two vent openings and the ceiling construction itself gave a total ceiling ELA of 826 cm^2 (128 in^2). In the first simulation, it was assumed that the roof cavity vent openings were sealed. In the second, it was assumed that the roof cavity contained vent openings consistent with the 1/300 rule. These two simulations are compared

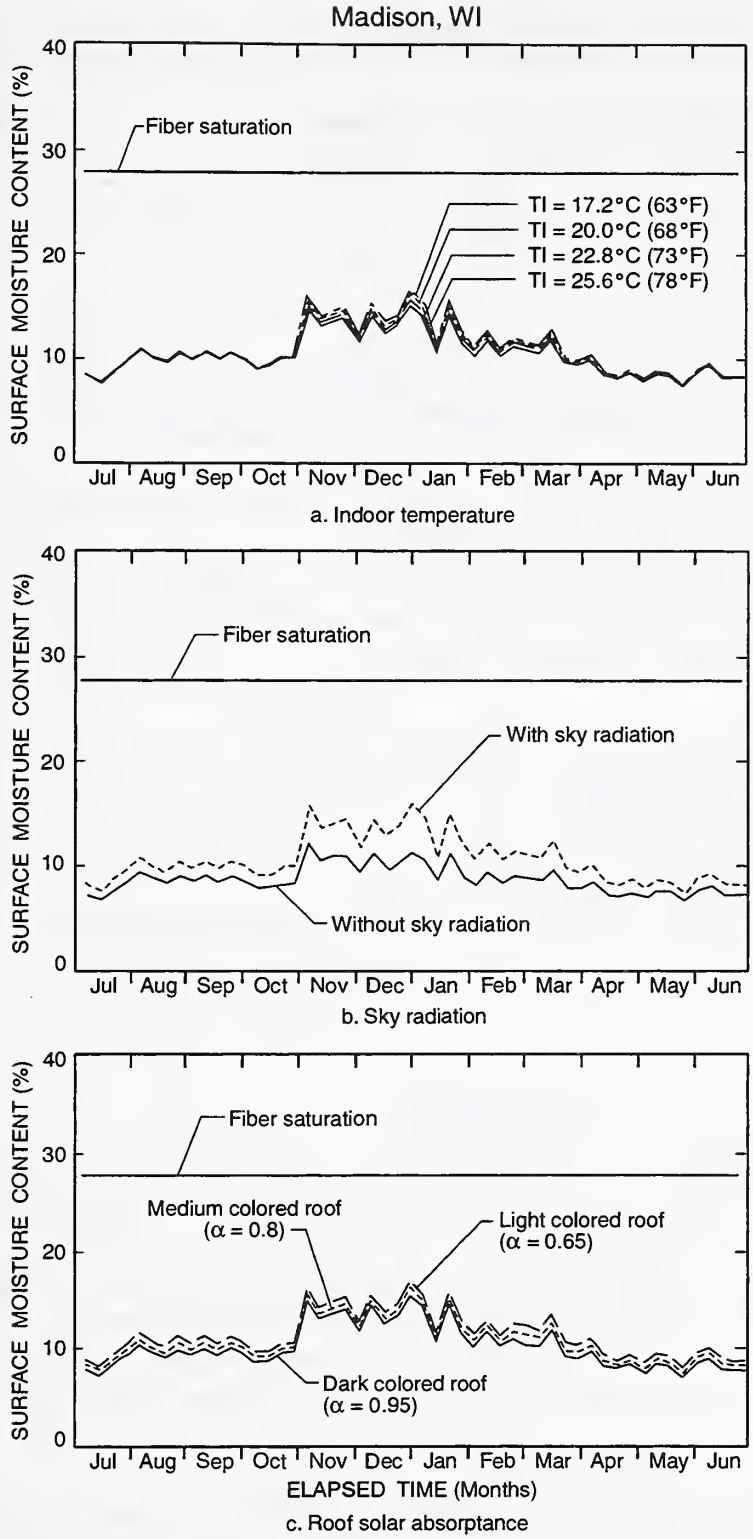

Fig. 17. Effect of other factors on the surface moisture content of north-sloping plywood roof sheathing for current practice house.

Table 4. Effect of Parameters on Roof Sheathing Moisture Content[1]	
Parameter	Diff. (% mc)
Passive Attic Ventilation (Roof Cavity Vents vs. None)	12
Mechanical Attic Ventilation (Wide Range)	13
Ceiling Vapor Retarder (with vs. without) * with Roof Cavity Vents * without Roof Cavity Vents	 1 3
Ceiling ELA with Passive Ventilation (Typical vs. None)	2
Indoor Humidification (with vs. without)	14
Indoor Moisture Generation Rate (Low vs. High)	5
Whole House ELA (Leakier vs. Tighter House)	2
Indoor Mechanical Ventilation (High vs. None)	3
Outdoor Climate Band	7
Indoor Temperature (Typical Range)	2
Sky Temperature (with vs. without)	4
Roof Color (Solar Absorptance Range: 0.65 to 0.95)	2

[1] The current practice house with a ceiling vapor retarder and 1/300 roof cavity vents was used as a baseline.

to that of the current practice house in Figure 18.

The roof sheathing moisture content, ceiling airflow rate, and indoor relative humidity for the above three simulations are given in Figures 18a, 18b, and 18c, respectively. In the house with two ceiling vents with no roof cavity vents, roof sheathing moisture content rose to 26% and approached fiber saturation (28%). The presence of the ceiling vents significantly increased the airflow from the house into the roof cavity (see Figure 18b), thereby transporting more moisture into the roof cavity. The additional whole house ventilation provided by the ceiling vents also lowered the indoor relative humidity (Figure 18c), which partially offset the effect of increased house airflow into the attic (Figure 18b).

As pointed out above, the two ceiling vents produced a significant increase in the airflow from the house into the roof cavity. From Figure 18b, the peak airflow from the house into the roof cavity is increased from 0.028 m^3/s (60 ft^3/min) to 0.041 m^3/s (86 ft^3/min), or a 43% increase. Space heating energy must be expended to heat additional incoming air. This imposes an annual space heating

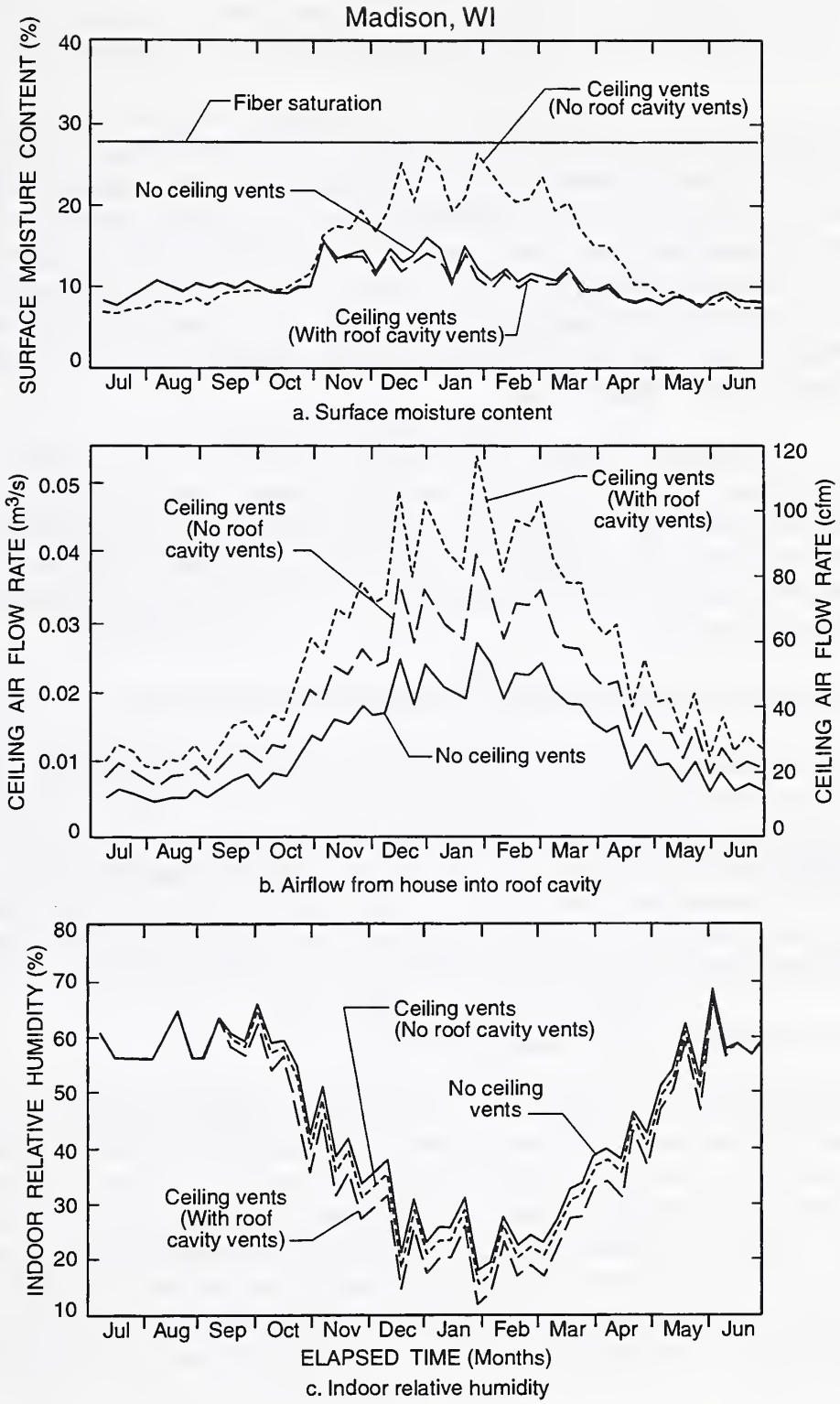

Fig. 18. Effect of ceiling vents on the moisture content of north-sloping plywood roof sheathing, airflow, and indoor relative humidity for current practice house.

energy penalty of 1520 kWh. At 6.4 cents per kWh, the annual cost to the homeowner for this additional space heating energy will be ninety-seven dollars ($97) in Madison, WI.

When roof cavity vents were added to the house with ceiling vents, the roof sheathing moisture content decreased approximately back to the level for the current practice house without ceiling vents (see Figure 18a). In this situation, the roof cavity vents removed a significant portion of the moisture transported by airflow. Another mitigating factor was that the presence of the roof cavity vents further increased the whole house ventilation, thereby giving rise to further reductions in indoor relative humidity (see Figure 18c). However, the roof cavity vents produced a further increase in the airflow from the house into the roof cavity. This, in turn, further increased the space heating energy penalty by an additional 810 kWh or fifty-two dollars ($52), giving a total increase of one hundred forty-nine dollars ($149).

In summary, the practice of providing whole house ventilation by installing ceiling vents without roof cavity vents has been shown to produce considerably higher roof sheathing moisture contents that approach fiber saturation. The problem of high sheathing moisture content may be overcome by installing roof cavity vents consistent with the 1/300 rule. However, the presence of the roof cavity vents further increased the whole house ventilation, which in turn produced an additional space heating energy penalty.

EFFECTIVENESS OF MOISTURE CONTROL PRACTICES IN COLD CLIMATES

In this section, the effectiveness of roof cavity vents consistent with the 1/300 rule is investigated for two worst case indoor relative humidity situations: a tight house having an ELA of 400 cm^2 (62 in^2) with a high moisture generation rate of 16.3 kg/day (36 lb/day) and a humidified house. These situations represent worst-case scenarios, but such extreme conditions are quite likely to exist within a fraction of the manufactured housing stock. It is crucial that moisture control practices work satisfactorily in houses operated under worst case humidity conditions. Consistent with the current HUD Standards, the house had a 57 ng/s·m^2·Pa (1 perm) ceiling vapor retarder.

Tight House with High Moisture Generation Rate

Separate computer simulations of this worst case house were carried out for the following levels of attic ventilation: no roof cavity vents, lower bound roof cavity vents, mean correlation roof cavity vents, and upper bound roof cavity vents (see Figure 6). The results are given in Figure 19.
For all three levels of roof cavity ventilation, the peak roof sheathing moisture content was below fiber saturation (28%). On the other hand, when no roof cavity vents are provided (upper curve), the roof sheathing moisture content rose considerably above fiber saturation during the winter and spring. This high roof sheathing moisture content may pose a risk of material degradation, although the roof sheathing dries out satisfactorily during warmer spring and summer periods when decay is more likely to occur.

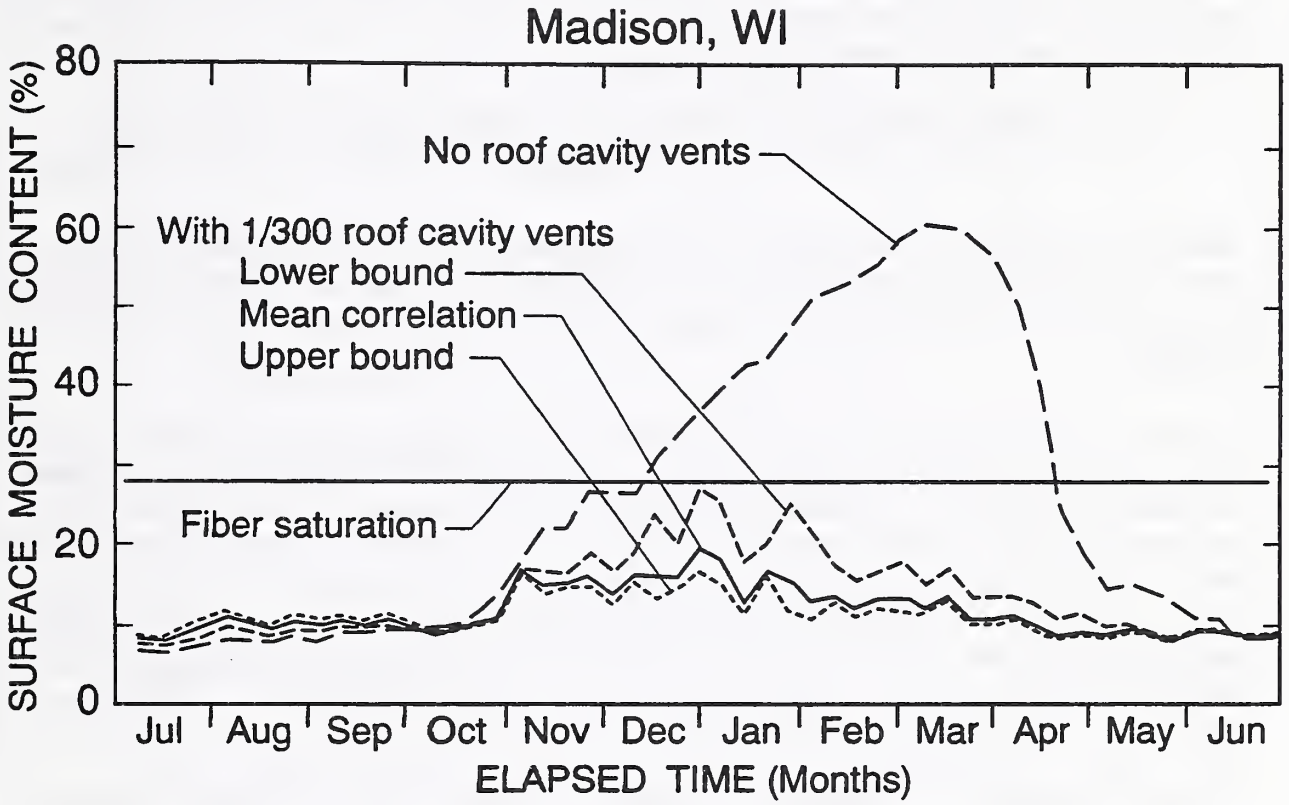

Fig. 19. Effectiveness of roof cavity vents in tight house with high moisture production rate.

Humidified House

A similar set of simulations was carried out for a humidified house. The results are given in Figure 20. When roof cavity vents are not provided (upper curve), moisture accumulated in the roof sheathing considerably above fiber saturation. Note that the high roof sheathing moisture contents do not extend significantly into spring and summer periods, when material degradation is likely to occur. For the three levels of roof cavity ventilation, the mean and upper bound curves were below fiber saturation, but the lower bound curve rose somewhat above fiber saturation. These results indicate that some humidified houses with roof cavity vents (consistent with the 1/300 rule) will experience roof sheathing moisture contents above fiber saturation. Therefore, it is recommended that manufactured houses not be humidified.

AN ALTERNATIVE ATTIC MOISTURE CONTROL PRACTICE IN COLD CLIMATES

Instead of providing attic ventilation, some building scientists have advocated sealing air leakage sites in the ceiling construction. This would reduce the airflow and moisture transport from the house into the roof cavity, and thereby maintain the roof sheathing moisture content below fiber saturation.

A series of computer simulations was conducted for the above worst case house without roof cavity vents. In these simulations, the ceiling ELA was varied from zero to 206 cm^2 (32 in^2). The results are depicted in Figure 21. Decreasing the ceiling ELA produced two separate effects. First, it decreased the airflow from the house into the roof cavity (see Figure 21b). Second, it increased the indoor relative humidity due to decreased whole house ventilation (see Figure 21c). The two results had an opposite effect on the roof sheathing moisture content. The overall effect is more gradual than expected (see Figure 21a). It is not until a ceiling ELA of 26 cm^2 (4 in^2) is reached that the roof sheathing moisture content is decreased sufficiently below fiber saturation. It is questionable whether such a low ceiling ELA is achievable in houses with roof cavities.

EFFECTIVENESS OF CURRENT MOISTURE CONTROL PRACTICES IN HOT AND HUMID CLIMATES

The model was next used to investigate the attic moisture performance of a current practice house in a hot and humid climate (Miami, FL). The current HUD Standards require that manufactured houses distributed in hot and humid climates have their attics ventilated consistent with the 1/300 rule. While a ceiling vapor retarder is not mandatory, it is none-the-less installed in many manufactured houses distributed to hot and humid climates.

For the current-practice house with a ceiling vapor retarder, separate computer simulations were carried out for cases with and without roof cavity vents. The results are given in Figure 22a. For both cases, the surface relative humidity above the ceiling vapor retarder rose above 80% and reached a peak during the summer. When roof cavity vents were present, the surface relative

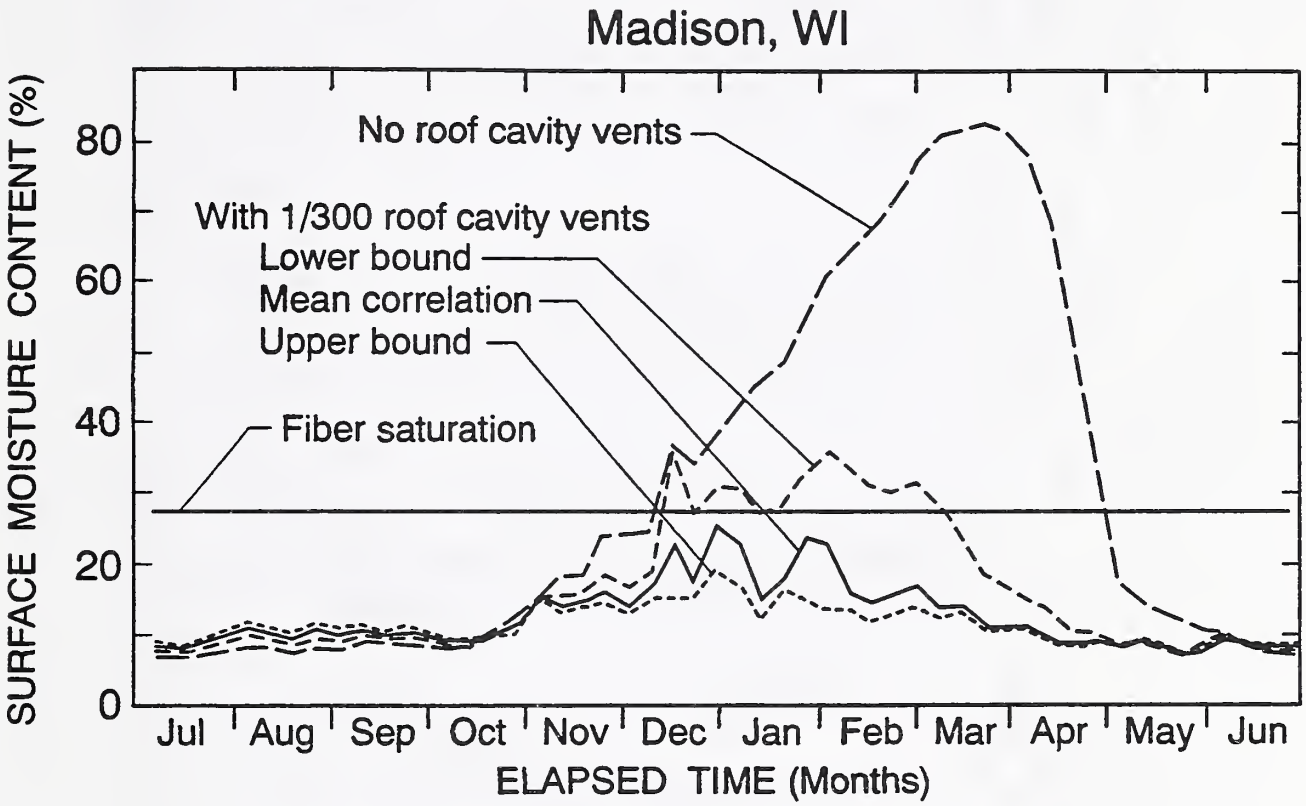

Fig. 20. Effectiveness of roof cavity vents in a humidified house.

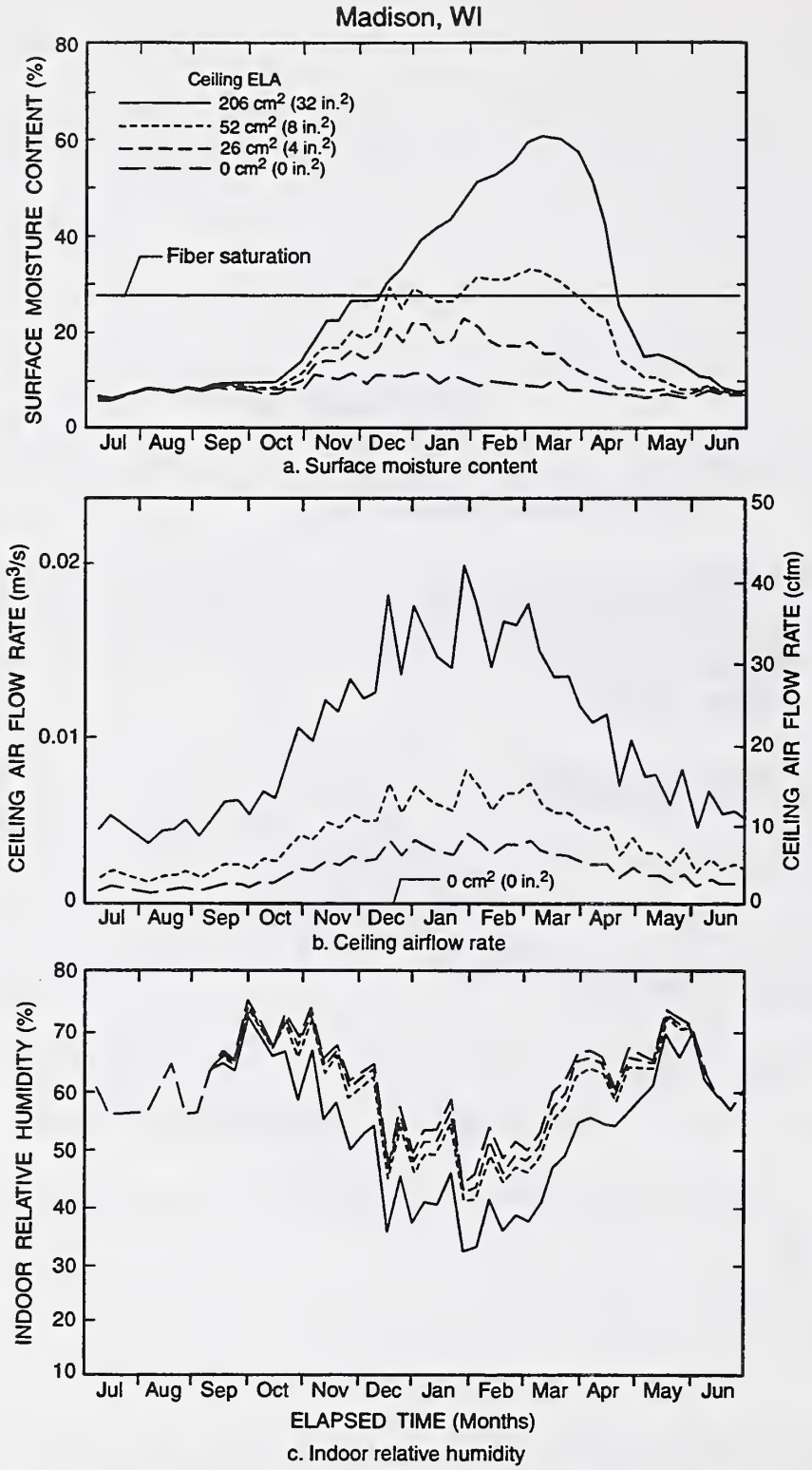

Fig. 21. Effectiveness of sealing air leakage paths in the ceiling construction of the tight house with high moisture generation rate as alternative moisture control practice.

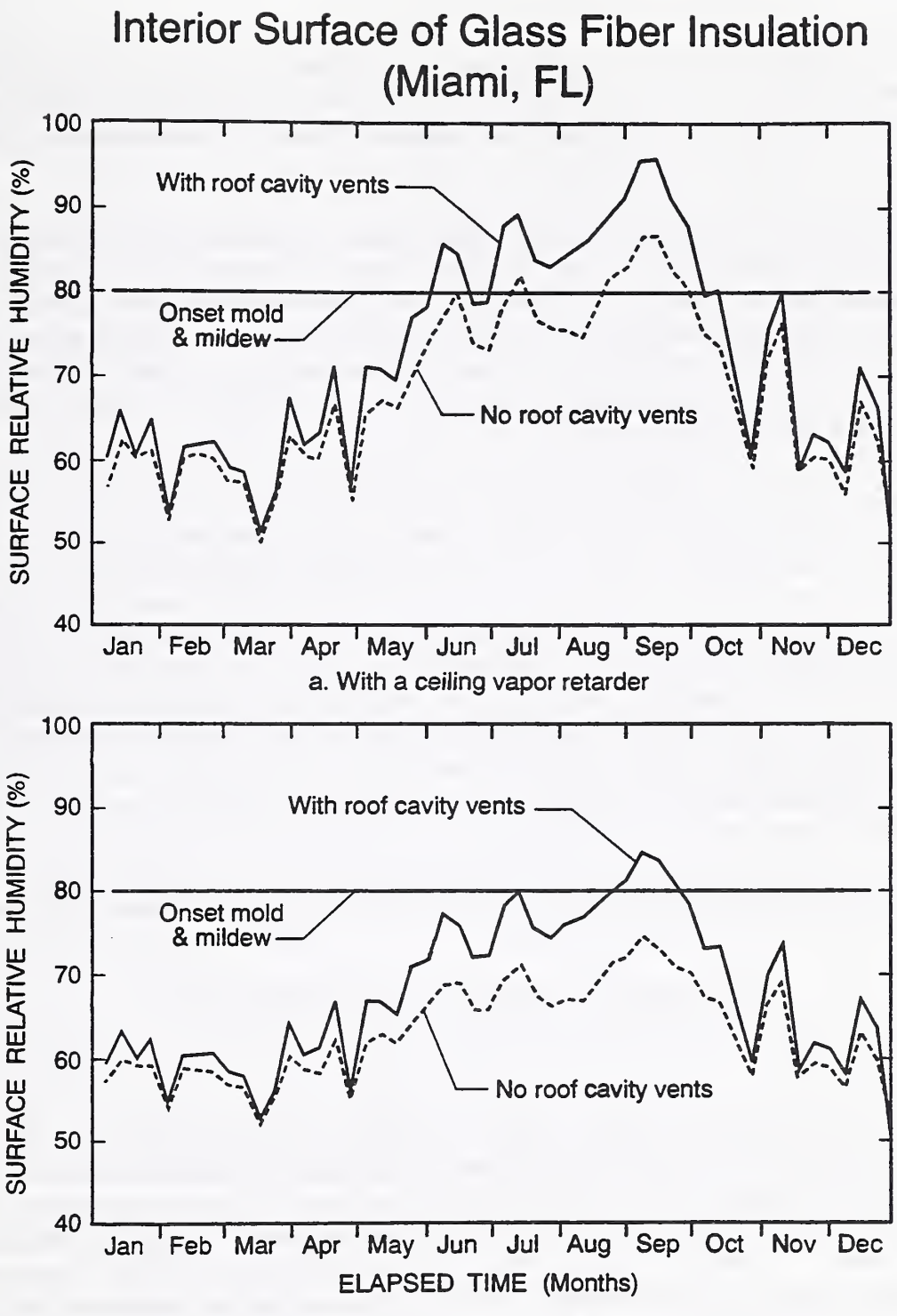

Fig. 22. Effectiveness of current HUD Standards moisture control practices in a hot and humid climate.

humidity was higher and above a relative humidity of 80% for a longer period of time. An explanation is that the roof cavity vents introduce more moisture (from the humid outdoor air) to the upper surface of the roof cavity insulation where it readily diffuses to the upper surface of the vapor retarder.

In Figure 22, the horizonal line depicts the critical relative humidity of 80% believed to coincide with mold and mildew growth. The International Energy Agency (IEA 1990) has published *Guidelines and Practices* (Volume 2) for preventing mold and mildew growth at building surfaces. This consensus document indicates that a monthly mean surface relative humidity above 80% is conducive to mold and mildew growth. Note that in the computer simulation with a ceiling vapor retarder and with roof cavity vents, the surface relative humidity rose above the critical 80% relative humidity for a 4-month summer period.

A similar pair of computer simulations were conducted for the same house without a ceiling vapor retarder. The results are given in Figure 22b. When roof cavity vents were not present, the roof cavity performed satisfactorily. That is, the surface relative humidity at the upper surface of the gypsum board remained below the critical 80% level. In this situation, the ceiling construction functions as a "pass through system" where moisture readily flows through it from the roof cavity to the indoor environment where it is removed by the air conditioning equipment. However, when roof cavity vents were present, the surface relative humidity rose above the critical 80% relative humidity for about a 1-month period. Before leaving this section, it is worth mentioning that the surface relative humidities in other parts of the construction were below the critical 80% level. In addition, the source of moisture in a hot and humid climate is the outdoor environment, as opposed to the indoor environment for cold climate applications.

The above results indicate that ceiling vapor retarders and roof cavity vents should not be installed in homes exposed to hot and humid climates.

RECOMMENDATIONS FOR FURTHER STUDY

Model Verification

A strong need exists to carry out a field experiment to verify the accuracy of the new MOIST Attic Model. The attic of a test house would be instrumented to measure the moisture content of the roof sheathing as a function of time. The outdoor boundary conditions (i.e., outdoor temperature, relative humidity, wind speed, wind direction, and horizontal solar radiation) would be measured as a function of time. In addition, special tests would be conducted to develop semi-empirical correlations that relate the attic air exchange rate to the outdoor wind speed and wind direction, and a separate semi-empirical correlation would be developed that predicts the airflow from the house into the attic. The moisture and heat transfer properties of the building materials would be independently measured. The moisture content of the roof sheathing would be measured as a function of time and compared to corresponding predicted values.

Roof Moisture Performance in Different U.S. Climates

The results of this report clearly show that similar roofs do not perform alike in different climates of the U.S. For example, utilizing attic ventilation and a ceiling vapor retarder is a good idea in northern cold climates, and yet it is not wise in hot and humid climates. Thus, HUD should not uniformly require attic ventilation and a ceiling vapor retarder in all climates of the U.S. as it now does. In order to clearly decide which distinct climatic regions should have which requirements and which should not, it would be worthwhile repeating the type of modeling undertaken in this report for a larger number of climates across the nation. For example, no modeling has been done for Alaska or Hawaii, or for mixed climates such as those of the southwest (Texas, Arizona, or southern California) or for mixed climates such as Arkansas or Tennessee. In addition, concurrent with examining moisture conditions, it would be worthwhile to look at energy use considerations (heat loss or gain through ceilings) in making decisions about HUD Standards revisions. The new model can be used to examine ceiling heat flux values for different roof conditions or constructions.

Uncertainties Regarding Attic Ventilation

The attic simulation model described and applied herein appears to be a valuable new tool for investigating potential attic moisture problems in manufactured housing. One weakness in the model is the lack of field data regarding leakage areas and especially the amount of air flow through attic cavities. The air exchange rate between the attic cavity and the outdoors was modeled using the LBL natural infiltration model (Sherman and Grimsrud 1980) with stack and wind coefficients obtained from measurements on twenty "site-built" houses. Typical manufactured housing is generally characterized by shallower roof pitches and lower attic volumes, as well as fairly airtight ceilings, and so the attic ventilation characteristics may be quite different than for site-built homes. Unfortunately, there are no known field data available for attic air exchange rates in manufactured homes. Such data are clearly needed.

In addition, better information is needed on the amount of unintentional roof leakage area in manufactured homes. There also is uncertainty about the typical ELA values of ceilings in manufactured homes. Moreover, the impact of the attic stack effect in hot and humid climates also warrants further investigation. It was neglected in this study based on cold climate Canadian data (Buchan, Lawton, Parent Ltd 1991). Yet attic modeling by Parker, Fairey, and Gu (1991) showed that buoyancy effects in attics in hot and humid climates may be important. Their analysis indicated that buoyancy was important in properly describing energy flows, but they did not focus on moisture transfer. These issues merit further investigation.

It would be most worthwhile to fit some manufactured homes with different commonly used attic ventilation systems and measure the air exchange rates with tracer gases over both short and long time periods. The field data could then be broken down to determine typical stack and wind coefficients for the LBL infiltration model for each type of ventilation. It also would be important to try to determine the impact of wind direction in such a study. Further, based on the results of this study, it would be most important to monitor the attics under conditions with high moisture

generation rates inside the homes that would most likely lead to adverse conditions in the attics or roof sheathing.

Finally, there are still some prominent building scientists who believe that roofs should not be ventilated. To unequivocally decide whether it is better to ventilate or not, it would be extremely worthwhile to test two manufactured houses side by side. One would have attic ventilation and the other would not. A comparison of their roof sheathing moisture contents would hopefully settle this issue once and for all.

Shingle Temperature

Building scientists and others associated with the building industry would like to know the effect of roof ventilation on the temperature of roof sheathing and roof coverings such as asphalt shingles. This is true for roofs with both open attics above flat ceilings and cathedral ceilings. The impact of roof ventilation and other factors such as the color of the exterior surface of the roof covering as well as the type of roof covering (e.g., asphalt shingles, shakes, tile, metal, etc.) is also of interest. The new MOIST Attic Model is well suited to help assess the impact of ventilation and other factors on roof sheathing temperatures. Thus, it is recommended that such modeling be undertaken.

SUMMARY AND CONCLUSIONS

A new mathematical model, called the MOIST Attic Model, was presented that predicts the transfer of moisture and heat in roof cavities. This model performs a heat and moisture balance on a roof cavity at hourly time steps, and includes the storage of moisture and heat at the construction layers. The airflow from the house through the ceiling construction into the roof cavity is predicted as a function of time using a stack-effect model. The ventilation rate of the roof cavity with outdoor air is predicted as a function of wind speed using a semi-empirical model with the roof ELA serving as an input. The relative humidity in the house below is permitted to vary during the winter and is predicted from a moisture balance of the whole building with the house ELA and indoor moisture production rate serving as inputs.

The above model was subsequently used to predict the performance of a double-wide manufactured house constructed in compliance with the current HUD Standards for manufactured housing. This current-practice house had an interior vapor retarder installed in its ceiling construction, and the roof cavity vents were installed consistent with the 1/300 rule. The moisture content of the plywood roof sheathing was predicted as a function of time of year, and the effect of a wide range of parameters on the peak moisture content was investigated. Most of the simulations were carried out in Madison (WI), although a series were carried out in different climates of the United States.

During the winter, the airflow from the house into the roof cavity was found to be the dominant mechanism for transporting moisture into the roof cavity. Water vapor diffusion was found to play a considerably less important role. Computer simulations of identical current-practice houses with and without a vapor ceiling retarder showed only a small difference in roof sheathing moisture

content. A ceiling vapor retarder was found to have a small effect because airflow from the house into the roof cavity was the dominant moisture transport mechanism. On the other hand, a much larger difference in roof sheathing moisture content occurred when the airflow from the house into the roof cavity was varied as a result of the ceiling air tightness.

Passive attic ventilation was found to be a very effective moisture control practice in non-humidified houses. When roof cavity vents consistent with the 1/300 rule were installed in the current-practice house in Madison (WI), (as required by the HUD standards), the peak moisture content of the plywood roof sheathing rose to only 16% during the winter. This peak moisture content was well below fiber saturation (28%). On the other hand, when the roof cavity vents were not present, the peak moisture content rose almost to fiber saturation. The analysis further revealed that the peak roof sheathing moisture content in houses without roof cavity vents can rise considerably above fiber saturation when the indoor relative humidity is elevated as in the case of a humidified house or a house having tighter construction and a high indoor moisture production rate. Roof sheathing moisture content above fiber saturation is believed to pose a risk of material degradation and shortened service life, especially if the plywood is wet in warm spring and summer periods.

The current HUD Standards permit attic mechanical ventilation at a rate of 0.00010 m^3/s per m^2 (0.02 ft^3/min per ft^2) of attic floor area to be used instead of roof cavity vents. When the model simulated the performance of a current practice house with this mechanical ventilation rate, the roof sheathing moisture content rose to fiber saturation during the winter. This was because the mechanical ventilation rate was too small. A mechanical ventilation rate of 0.0005 m^3/s per m^2 (0.1 ft^3/min per ft^2) of attic floor area was found to provide satisfactory performance. It is recommended that HUD revise the specified mechanical rate for roof cavities.

The computer simulations showed that houses with higher indoor relative humidity have higher roof sheathing moisture content. Elevated indoor relative humidity occurs in houses that have high moisture production rates, tight building envelopes, and/or humidification. When the current practice house was humidified at an indoor relative humidity of 45% during the winter in Madison (WI), moisture content of the north sloping plywood roof sheathing rose to a peak of 25% and approached fiber saturation (28%). When the roof cavity vents were not present, the model predicted roof sheathing moisture contents considerably above fiber saturation in the humidified house. Such wet roof sheathing could potentially degrade.

The practice of providing whole house ventilation by ventilating indoor air (through ceiling vents) into a roof cavity without roof cavity vents was found to cause elevated roof sheathing moisture contents that approached fiber saturation in houses located in Madison, WI. The problem of high roof sheathing moisture content is somewhat diminished by lower indoor relative humidities produced by the additional whole house ventilation. Another negative attribute is that this practice imposes a space heating energy penalty on the house. Over the course of the heating season, the authors calculated that 1,520 kWh would be required to heat incoming ventilation air in an electrically heated house. At 6.4 cents per kWh, the energy penalty for providing this additional whole house ventilation would be ninety-seven dollars ($97) per year.

The coldness of the outdoor climate was found to have much less effect on the sheathing moisture content than reported in a previous study. In the present study, the indoor relative humidity was permitted to vary during the winter and was calculated from a moisture balance of the whole building. The roof sheathing moisture contents tended to lie within a narrow range. In the previous study, the indoor relative humidity was maintained at a constant level in all the simulations, and the roof sheathing moisture content increased markedly with the coldness of the outdoor climate. The effect of climate is diminished in the present study because lower indoor relative humidities occur in colder climates, which decreases the indoor potential (i.e. water-vapor pressure) for moisture transport into the roof cavity.

In non-humidified houses, the current moisture control practices given in the HUD Standards (i.e, installing an interior vapor retarder in the ceiling construction and installing roof cavity vents consistent with the 1/300 rule) were found to be effective in cold climates. That is, the peak moisture content of the roof sheathing was always well below fiber saturation in non-humidified houses of tighter construction with high indoor moisture generation rates. However, in humidified houses, some houses with roof cavity vents may experience roof sheathing moisture contents above fiber saturation during the winter months. Even in those cases, the roof sheathing dried out satisfactorily during the spring and early summer when wood temperatures are high enough for decay to occur. Thus, structural damage is unlikely.

These same moisture control practices did not result in acceptable performance in hot and humid climates. When a vapor ceiling retarder was present, moisture from the outdoor environment accumulated at its upper surface where the relative humidity rose above the critical 80% level conducive to mold and mildew growth. Higher surface relative humidities at the vapor retarder occurred in houses with roof cavity vents. In houses exposed to hot and humid climates, it may be wise not to install a ceiling vapor retarder and roof cavity vents. It is particularly important to avoid installing a ceiling vapor retarder.

It is recommended that field studies be conducted to experimentally corroborate the above theoretical results prior to making revisions to the HUD Standards for manufactured housing.

ACKNOWLEDGMENTS

The authors thank William Freeborne of the Division of Affordable Housing, Research, and Technology of the U.S. Department of Housing and Urban Development for funding this project and making many helpful suggestions during the review of the report. The authors would like to thank Walter Rossiter and Dale Bentz for providing many helpful suggestions during the review of the report. The authors would also like to thank Paula Svincek for preparing this manuscript for publication, and Ray Mele for preparing the figures for publication.

NOMENCLATURE

Symbol	SI Units	English Units	Definition
A_f	m^2	ft^2	House floor area
A_n	m^2	ft^2	Area of surface n
B_1, B_2, B_3	-	-	Constants in sorption isotherm equation
c	J/kg·K	Btu/lb·°R	Specific heat
C_1, C_2, C_3	-	-	Constants in permeability equation
$C_{v,c}$	$(L/s)^2 \cdot cm^{-4} \cdot (m/s)^{-2}$	$cfm^2/in.^4 \cdot mph^2$	Wind coefficient for roof cavity
$C_{v,h}$	$(L/s)^2 \cdot cm^{-4} \cdot (m/s)^{-2}$	$cfm^2/in.^4 \cdot mph^2$	Wind coefficient for house
$C_{\Delta T,c}$	$(L/s)^2 \cdot cm^{-4} \cdot K^{-1}$	$cfm^2/in.^4 \cdot °F$	Stack coefficient for roof cavity
$C_{\Delta T,h}$	$(L/s)^2 \cdot cm^{-4} \cdot K^{-1}$	$cfm^2/in.^4 \cdot °F$	Stack coefficient for house
D_γ	m^2/s	ft^2/h	Liquid diffusivity
E	-	-	Emittance factor
h_{lv}	J/kg	Btu/lb	Latent heat of vaporization
$h_{c,i}$	$W/m^2 \cdot K$	$Btu/h \cdot ft^2 \cdot °R$	Convective heat transfer coef. at inside surf.
$h_{c,n}$	$W/m^2 \cdot K$	$Btu/h \cdot ft^2 \cdot °R$	Convective heat transfer coef. at surface n
$h_{c,o}$	$W/m^2 \cdot K$	$Btu/h \cdot ft^2 \cdot °R$	Convective heat transfer coef. at outside surf.
$h_{r,i}$	$W/m^2 \cdot K$	$Btu/h \cdot ft^2 \cdot °R$	Radiative heat transfer coef. at inside surf.
$h_{r,o}$	$W/m^2 \cdot K$	$Btu/h \cdot ft^2 \cdot °R$	Radiative heat transfer coef. outside surf.
H_c	m	ft	Stack height for roof cavity
H_h	m	ft	Stack height for house
H_{sol}	W/m^2	$Btu/h \cdot ft^2$	Incident solar radition onto a surface
k	W/m·K	Btu/h·ft·°R	Thermal conductivity
K	kg/m·s·Pa	lb/ft·h·inHg	Hydraulic conductivity
L_c	m^2	ft^2	Effective leakage area for ceiling construction
L_e	m^2	ft^2	Effective leakage area for stack effect airflow
L_h	m^2	ft^2	Effective leakage area for whole house
L_w	m^2	ft^2	Effective leakage area for house exterior walls
L_r	m^2	ft^2	Effective leakage area for roof construction
m_n	$kg/m^2 \cdot s \cdot Pa$	$lb/ft^2 \cdot h \cdot inHg$	Mass transfer coefficient at surface n
$M_{e,i}$	$kg/m^2 \cdot s \cdot Pa$	$lb/ft^2 \cdot h \cdot inHg$	Effective inside surface permeance
$M_{f,i}$	$kg/m^2 \cdot s \cdot Pa$	$lb/ft^2 \cdot h \cdot inHg$	Air film permeance at inside surface
$M_{p,i}$	$kg/m^2 \cdot s \cdot Pa$	$lb/ft^2 \cdot h \cdot inHg$	Paint permeance at inside surface
n	-	-	Hourly summation index
N	-	-	Current hour
p_l	Pa	inHg	Capillary pressure
p_v	Pa	inHg	Water vapor pressure
$p_{v,i}$	Pa	inHg	Water vapor pressure of indoor air
$p_{v,c}$	Pa	inHg	Water vapor pressure of cavity air
$p_{v,n}$	Pa	inHg	Water vapor pressure at surface n
Δp_r	Pa	inHg	Stack-effect reference pressure (4 Pa)
Δp_t	Pa	inHg	Total stack-effect pressure
t	s	h	Time
T	°C	°F	Temperature

Symbol	SI Units	English Units	Definition
T_c	°C	°F	Cavity air temperature
T_i	°C	°F	Indoor temperature
T_m	°C	°F	Mean temperature between the surface and sky
$T_{s,n}$	°C	°F	Temperature of surface n
T_{sky}	°C	°F	Sky temperature
T_o	°C	°F	Outdoor air temperature
v	m/s	mi/h	Average wind speed
$\dot{V}_c$	m^3/s	ft^3/min	Outdoor cavity ventilation rate
$\dot{V}_{h\rightarrow c}$	m^3/s	ft^3/min	Airflow rate from house to cavity
$\dot{V}_{h,m}$	m^3/s	ft^3/min	House mechanical ventilation rate
$\dot{V}_{h,n}$	m^3/s	ft^3/min	House natural ventilation rate
$\dot{V}_{h,t}$	m^3/s	ft^3/min	Total house ventilation rate
y	m	ft	Distance
$\dot{W}$	kg/s	lb/h	Moisture generation rate
Z(n)	-	-	Exponential weighting factors
γ	kg/kg	lb/lb	Moisture content on dry mass basis
ϵ_M	-	-	Convergence criteria for moisture solution
ϵ_T	-	-	Convergence criteria for thermal solution
κ	$kg/s \cdot m^2$	$lb/h \cdot ft^2$	Sorption constant per unit floor area
ρ_a	kg/m^3	lb/ft^3	Air density
ρ_d	kg/m^3	lb/ft^3	Dry material density
σ	$W/m^2 \cdot K^4$	$Btu/h \cdot ft^{2\circ} \cdot R^4$	Stefan-Boltzmann constant
μ	kg/m·s·Pa	lb/h·ft·inHg	Water vapor permeability
τ	s	h	Moisture storage time constant
ϕ	-	-	Relative humidity
ϕ_i	-	-	Indoor relative humidity
$\phi_{i,\tau}$	-	-	Indoor hygric memory
ω_c	kg/kg	lb/lb	Cavity air humidity ratio
ω_i	kg/kg	lb/lb	Indoor air humidity ratio
ω_o	kg/kg	lb/lb	Outdoor air humidity ratio

REFERENCES

ASHRAE. 1993. 1993 ASHRAE Handbook - Fundamentals, Atlanta: American Society of Heating, Refrigerating and Air-Conditioning Engineers, Inc.

Bliss, R.W. 1961. "Atmospheric Radiation Near the Surface of the Ground." *Solar Energy*, 5,103.

Buchan, Lawton, Parent Ltd. 1991. "Survey of Moisture Levels in Attics." Research Report BLP File No. 2497 submitted to Canada Mortgage and Housing Corporation; Ottawa, Ontario.

Burch, D.M. and Thomas, W.C. 1992. "An Analysis of Moisture Accumulation in a Wood Frame Wall Subjected to Winter Climate," Proceedings of Thermal Performance of the Exterior Envelopes of Buildings V, ASHRAE/DOE/BTECC Conference, Dec. 7-10, Clearwater Beach, FL.

Burch, D.M., Thomas,W.C., and Fanney, A.H. 1992. "Water Vapor Permeability Measurements of Common Building Materials." *ASHRAE Transactions*, 98(2).

Burch, D.M. 1995. "An Analysis of Moisture Accumulation in the Roof Cavities of Manufactured Housing," Airflow Performance of Building Envelopes, Components, and Systems, ASTM STP 1255, American Society of Testing and Materials, Philadelphia, pp.156-177.

Carrol, J.A. 1980. "An 'MRT Method' of Computing Radiant Energy Exchange in Rooms." *Proceedings of the Second Systems Simulation and Economics Analysis Conference*, San Diego, CA, pp. 903-917.

Climatic Atlas of the United States. 1983. National Oceanic and Atmospheric Administration; U.S. Department of Commerce, June.

Crow, L.W. 1981. "Development of Hourly Data for Weather Year for Energy Calculations (WYEC)." *ASHRAE Journal*, 23(10): 34-41.

Duffie, J.A. and Beckman, W.A. 1991. Solar Engineering of Thermal Processes, Second Edition. John Wiley & Sons, Inc.

Edwards, J.R. 1996. "Equilibrium Moisture Content Measurement for Porous Building Materials at Various Temperatures." M.S. Thesis, Mechanical Engineering Department, Virginia Polytechnic Institute & State University, May.

Greenspan, L. 1977. "Humidity Fixed Points of Binary Saturated Aqueous Solutions." *Journal of Research*, National Bureau of Standards (now National Institute of Standards and Technology), 81A(1): 89-96.

Hadley, D.L. and Bailey, S.A. 1990. "Infiltration/Ventilation Measurements in Manufactured Homes - Residential Construction Demonstration Program." Pacific Northwest Laboratory Report No. PNL-7494 UC-350, August.

Hedlin, C.P. 1967. "Sorption Isotherms of Twelve Woods at Subfreezing Temperatures." *Forest Products Journal*, Vol. 17, No. 12.

International Energy Agency. 1990. Annex XIV, Condensation and Energy. Volume 2. *Guidelines and Practices*. August.

Olson, J., Schooler, S., and Mansfield, M. 1993. "Tri State Homes: a Case Study of Liability for Defective Homes which Created Unhealthy Environments Causing Personal Injuries." *Proceedings of the International Conference on Building Design, Technology & Occupant Well-Being in Temperate Climates*. Brussels, Belgium, February.

Palmiter, L. and Bond, T. 1991. "Interaction of Mechanical Systems and Natural Infiltration," *Proceedings of AIVC Conference on Air Movement and Ventilation Control Within Buildings*, Ottawa, Ontario, Canada.

Palmiter, L., Bond, T., Brown, I. Baylon, D. 1992. "Measured Infiltration and Ventilation in Manufactured Homes: Residential Construction Demonstration Project Cycle II", prepared for Bonneville Power Administration, April 28.

Parker, D.S., Fairey, P.W., and Gu, L. 1991. "A Stratified Air Model For Simulation of Attic Thermal Performance." *Insulation Materials, Testing and Applications*, Vol. 2, ASTM STP 1116. American Society for Testing and Materials, Philadelphia, PA.

Parker, D.S., McIlvaine, J.E.R., Barkaszi, Jr. S.F., and Beal, D.J. 1993. "Laboratory Testing of Reflectance Properties of Roofing Materials." Florida Solar Energy Center, FSEC-CR-67O-93, August.

Pedersen, C.R. (now Carsten Rode). 1990. "Combined Heat and Moisture Transfer in Building Constructions." Report No. 214. Technical University of Denmark. September.

Richards, R.F. 1992. "Measurement of Moisture Diffusivity for Porous Building Materials." *Proceedings of ASHRAE/DOE/BTECC Conference on Thermal Performance of the Exterior Envelopes of Buildings V*, Clearwater Beach, FL, Dec. 7-10.

Richards, R.F., Burch, D.M., and Thomas, W.C. 1992. "Water Vapor Sorption Measurements of Common Building Materials." *ASHRAE Transaction, 98(2).*

Sherman, M.H. and Grimsrud, D.T. 1980. "Infiltration-Pressurization Correlation: Simplified Physical Modeling." *ASHRAE Transaction*, 86(2):778.

Sherwood, G.E. 1994. "Moisture-Related Properties of Wood and the Effect of Moisture on Wood and Wood Products." *Moisture Control in Buildings,* ASTM Manual Series MNL 18. H. Trechsel (Ed.). American Society for Testing and Materials, Philadelphia, PA.

TenWolde, A. 1994. "Ventilation, Humidity, and Condensation in Manufactured Houses during Winter." *ASHRAE Transactions*, Volume 100, Part 1.

Threlkeld, J.L. 1970. Thermal Environmental Engineering. Prentice-Hall, New York. pp. 196-198.

Tsongas, G.A. 1990. "The Northwest Wall Moisture Study: A Field Study of Excess Moisture in Walls and Moisture Problems and Damage in New Northwest Homes." U.S. DOE/Bonneville Power Administration, Portland, OR, Report No. DOE/BP-91489-1, June.

Tsongas, G., Burch, D., Roos, C., and Cunningham, M. 1995. "A Parametric Study of Wall Moisture Contents Using a Revised Variable Indoor Relative Humidity Version of the "MOIST" Transient Heat and Moisture Transfer Model." *Proceedings of the Thermal Performance of the Exterior Envelopes of Buildings VI.* , Clearwater Beach, FL, Dec. 4-8.

U.S. Department of Housing and Urban Development, 1994. "Manufactured Home Construction and Safety Standards." Code of Federal Regulations, Title 24, Part 3280.

Walton, G.N. 1994. "CONTAM93 User Manual." NISTIR 5385. National Institute of Standards and Technology, March.